Title of Thesis

"Studies on the facts of the loss of MMP3 on tumoroid formation and the integrity of extracellular vesicles"

"MMP3 の欠損が腫瘍形成と細胞外小胞の完全性に及ぼす影響に関する研究"

September 2020

Eman Ahmed Mohamed Mohamed Taha

Graduate School of Natural Science and Technology
Okayama University

Doctoral Program

OKAYAMA UNIVERSITY

Acknowledgment

First, I would like to express my sincere gratitude to my supervisor **Dr. Ayano Satoh** for the valuable support, understanding, and thoughtful comments and recommendations on this dissertation. Thank you for supporting me to find a friendly atmosphere where I can learn and grow. I would like to express my deep gratitude to **Dr. Takanori Eguchi** for his valuable and constructive suggestions during the planning and development of this research work. He helped me a lot in editing and revising the manuscript as well as teaching me how to use and represent my data. Besides, he allowed me to improve my academic writing skills, thanks to him I was able to build such a good publication record.

My grateful thanks are also extended to **Dr. Chiharu Sogawa** for her advice and assistance in designing the experimental protocols, teaching me how to use different instruments and programs. Also, for her help in visualizing the data, editing and revising the manuscript, and paying the publication fees. I appreciate your kindness, support, and personal approach. Words cannot express how grateful I am for the kindness and generosity of **Prof. Dr. Kuniaki Okamoto**. Thank you for your valuable support, insightful discussions, and accepting me as a member of your lab.

Besides my advisors, I would like to thank the rest of my thesis committee: **Prof. Dr. Takashi Otsuki** and **Prof. Dr. Hiroshi Tokumitsu** for their insightful comments, and valuable suggestions. My special thanks are extended to **Prof. Dr. Masaharu Seno** for allowing me to study in Japan and to **Dr. Maram Hussein** for her warm welcome as well as to **Prof. Dr. Heiichiro Udono** for being considerate and kind towards me. Also, for allowing me to visit his lab and his explanation of various immunological techniques. Additionally, I am grateful to the help provided by **Ms. Sarah Chikako**, and **Dr. Sabina Mahmoud** as well as **Dr. Mariko Muzuka**.

I am particularly grateful for the assistance given by **Dr. Yuka Okusha**, **Dr. Hotaka Kawai**, **Prof. Dr. Satoshi Kubota**, **Prof. Dr. Masaharu Takigawa**, **Prof. Dr. Hitoshi Nagatsuka**, **Dr. Eriko Aoyama**, **Dr. Abdellatif Elseoudi**, **Mr. Haruo Urata**, **Ms. Kazuko Kobayashi**, May Wathone Oo, my lab mates; **Dr. Kisho Ono**, **Yanyin Lu**, **Feng Yunxia**, **Penggong Wei**, and **Toshiki Nara** for their valuable assistance and contribution to my research project.

Besides, the scholarship provided by Egypt-Japan Education Partnership **(EJEP)** agency, took away the financial burden, allowing me to focus on my study. A special appreciation is extended to **Prof. Dr. Hany A. El-Shemy**; Cultural Counselor, and **Dr. Hanem Ahmed**; Cultural Attache, **Mr. Fathy Dawoud** and **Ms. Keiko Morishita** from the Culture, Education, and Science Bureau in Tokyo, as well as to the members of the Ministry of Higher Education and Scientific Research in Cairo for their support and help.

I am grateful to all professors and colleagues from the Biochemistry department, Faculty of Science in Cairo for their support and encouragement. Especially, I am grateful **to Prof. Dr. Ibrahim Kamal**, **Prof. Dr. Mohamed Ragaa**, **Prof. Dr. Nadia Abdallah, Prof. Dr. Magda Kamal, Prof. Dr. Tahany Abd El-Moneam** (who passed away before I visited Japan), **Prof. Dr. Fawzya Ashoor**, **Dr. Rania Hassan**, **Dr. Elham Abdel-Badiea, Dr. Walaa Elabd, Dr. Hayam Rushdy** for their encouragement and valuable support.

Besides, I would like to express my very great appreciation to **Dr. Hamdy Aly and** his wife **Mrs. Basma Fakery**, for being so kind, very supportive, and helping me out when I needed it.

Finally, I must express my very profound gratitude to **my parents, sisters, and brothers** for providing me with unfailing support and continuous encouragement. Thank you so much for being there for me and for believing in me. This accomplishment would not have been possible without your sincere prayers during these difficult times. Thank you.

Eman A. Taha

Abbreviations

EVs	Extracellular vesicles
MV	Microvesicles
MVBs	Multivesicular endosomes
MHC	Major histocompatibility complex proteins
ILVs	Intraluminal vesicles
Rab	The Rab family is part of the Ras superfamily of small GTPases.
ESCRT	The endosomal sorting complex required for transport
TSG101	Tumor Susceptibility 101
HSP	Heat shock proteins
TME	Tumor microenvironment
CAFs	Cancer-associated fibroblasts
VEGFA	Vascular endothelial growth factor-A
CXCL	C-X-C motif chemokine
IL-6	Interleukin 6
ECM	Extracellular matrix
TGF-β1	Transforming growth factor-beta
CRC	Colorectal cancer
EGFR	Epidermal growth factor receptor
MET	Tyrosine-protein kinase Met
tdTomato	Palmitoylation signal-fused fluorescent proteins such as tandem dimer Tomato
EGFP	Enhanced green fluorescence protein
MMPs	Metalloproteinases
PEX	A hemopexin-like repeat domain
IGFBP	Insulin-like growth factor-binding protein
IGFR	Insulin-like growth factor 1receptor

HB-EGF	Heparin-binding epidermal growth factor-like growth factor
EGFR/ERBB	Epidermal growth factor receptor
FGF-2	Fibroblast growth factor- 2
EMT	Epithelial-mesenchymal transition
MET	Mesenchymal-epithelial transition
ZEB	Zinc finger E-box-binding homeobox protein
SNAIL	Zinc finger transcriptional repressor
ESCC	Esophageal squamous cell carcinoma
CCN2/CTGF	Connective tissue growth factor
IFN-α	Interferon-alpha
NFKIBA	Nuclear factor-κB inhibitor alpha
NLS	Nuclear localization signaling sequence
PARP	Poly (ADP-ribose) polymerase
FADD	FAS-associated death domain protein
Bax	BCL2 associated X
Bcl-xs	B-cell lymphoma-shorter form
XRCC1	X-ray repair cross-complementing protein
RANKL	Receptor activator of nuclear factor kappa B ligand
VEGFR-1TK	Vascular endothelial growth factor receptor 1 tyrosine kinase
2D	Two-dimensional
3D	Three-dimensional
NCP	NanoCulture plates
ULA	Ultra-low attachment

List of Figures

List of Tables

1. Introduction

1.1. Classification of extracellular vesicles (EVs)

Communications of cancer cells with each other or with neighboring cells or cells at distant sites are crucial for tumor proliferation and dissemination (Jakhar and Crasta 2019). Extracellular vesicles (EVs) are lipid bi-layered vesicles that are released from almost all cells under physiological and pathological conditions. EVs play a crucial role in intercellular communications at local and distant sites (Yáñez-Mó et al. 2015). These small vesicles carry various molecular cargo such as; nucleic acids (DNA, RNA), proteins, lipids, and metabolites that could be transferred into the recipient cells leading to genetic alterations and reprogramming of these cells (Raposo and Stoorvogel 2013; Colombo, Raposo, and Théry 2014; Yáñez-Mó et al. 2015; Eman A Taha, Ono, and Eguchi 2019).

According to the vesicle size, EVs are mainly classified into three categories; exosomes (50-200 nm), ectosomes are also known as microvesicles (MV) (100-500 nm), and apoptotic bodies (1-10 μm) (Andreola et al. 2002; Janowska-Wieczorek et al. 2005; Lawson et al. 2016). In addition to this heterogenous population, other vesicles have been reported including., oncosomes (Al-Nedawi et al. 2008; Rak 2013; Choi et al. 2019), large oncosomes (1-10 μm) (Di Vizio et al. 2012; Vagner et al. 2018), matrix vesicles (Mebarek et al. 2013; Chen et al. 2016; Schmidt et al. 2016), migrasomes (50 nm to 3 μm) (Ma et al. 2015; Huang et al. 2019), exopheres (~4 μm), exomeres (~35 nm), and bacterial outer membrane vesicles (OMV) (Raposo and

Stoorvogel 2013; Kim et al. 2017; Van Niel, D'Angelo, and Raposo 2018; Coelho et al. 2019).

Notably, EVs are heterogeneous populations, so there is no unanimous consensus on the nomenclature of them. General terms such as "exosomes" and "microvesicles" have been broadly used. The International Society for Extracellular Vesicles (ISEV) proposed to use the term EVs in general to describe vesicles naturally released from the cells and surrounded by a lipid bilayer unless authors can establish specific markers of subcellular origin with a description based of physical characteristics, such as size (Théry et al. 2018). Thus, I will use the general term EVs, and classify it into small and large EVs based on the size of vesicles.

1.2. Biogenesis and characteristics of EVs

Exosomes are vesicles of endosomal origin. Their biogenesis starts with the inward budding of the cellular plasma membrane, internalization of extracellular ligands from the cell surface (e.g., growth factor receptors) or from the Golgi apparatus (e.g., MHC class-II molecules) forming early endosomes (Babst 2005; Trajkovic et al. 2008; Fader and Colombo 2009; Babst 2011; Colombo et al. 2013; Jakhar and Crasta 2019; Eman A Taha, Ono, and Eguchi 2019). Early endosomes mature into late endosomes. After that, the endosomal membrane undergoes a second inward (intraluminal) budding to generate smaller vesicles within the late endosome lumen to form multivesicular bodies (MVBs), which are carrying various bioactive molecules such as proteins, lipids, and nucleic acids of the parent cell. Finally, MVBs either fuse with lysosomes to be degraded or fuse with the plasma membrane thereby releasing the intraluminal

vesicles, termed exosomes, into the extracellular space (Figure 1) (Trajkovic et al. 2008; Fader and Colombo 2009; Babst 2011; Colombo et al. 2013; Jakhar and Crasta 2019; Eman A Taha, Ono, and Eguchi 2019). Once generated within the MVB, the release exosomes into the extracellular space are mediated by small transport GTPases molecules such as; Rab27A, Rab11, and Rab31, which can collaborate with SNARE (a soluble N-ethylmaleimide sensitive factor attachment protein receptor) proteins to fuse the MVB membrane with their target membrane (Bobrie et al. 2011).

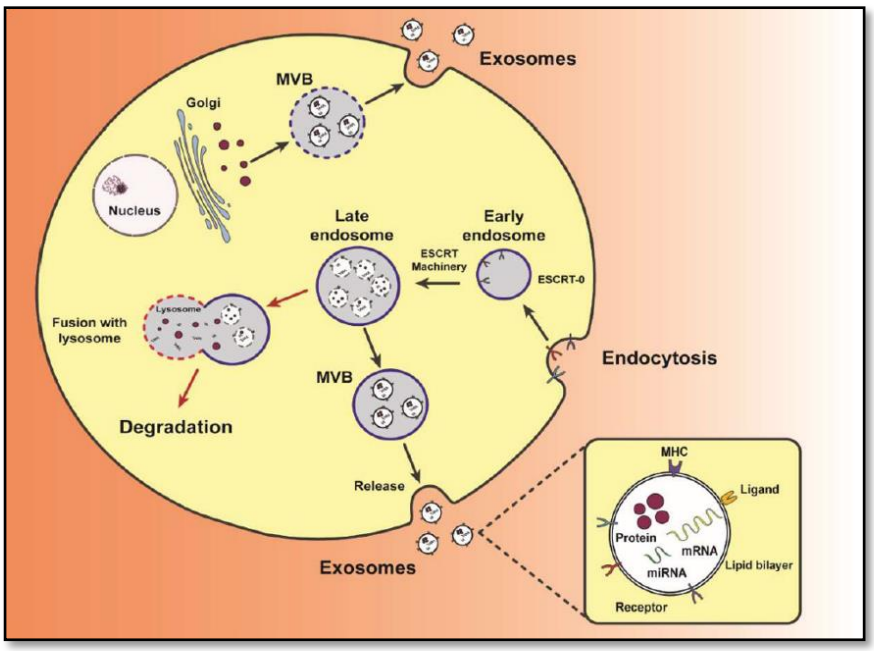

Figure 1. Schematic representation of exosome biogenesis and release (Jakhar and Crasta 2019).

It is worth noting that the formation of exosomes within the MVBs occurs by the endosomal sorting complex required for transport (ESCRT)-dependent machinery and ESCRT-independent mechanisms. Four distinct ESCRT protein complexes have been

identified (ESCRT-0, -I, -II, and -III). The ESCRT-dependent biogenesis starts with the inward budding of the cell membrane with aid from ESCRT-0 to produce early endosomes. The other ESCRT complexes contributing to the packaging of exosome contents into late endosomes. Whereas, the ESCRT-independent biogenesis involves the packaging of proteins from the Golgi into exosomes within MVBs and discharged into the extracellular milieu in the absence of ESCRT machinery (Babst 2011; Jakhar and Crasta 2019).

In general, EVs are characterized by their cup-shaped lipid bilayers structure under the electron microscope (Szatanek et al. 2017). Despite the absence of specific protein markers to distinguish between the different subtypes of EVs, the protein profiles of MVs, exosomes, and apoptotic bodies are different due to their different routes of formation (F. T. Borges, Reis, and Schor 2013; Yáñez-Mó et al. 2015; Mikołaj P Zaborowski et al. 2015). For instance, the membrane of Exosome contains cholesterol, sphingomyelin, phosphatidylinositol, ceramide, and lipid rafts (Théry, Ostrowski, and Segura 2009; Ciardiello et al. 2016; Tamkovich, Tutanov, and Laktionov 2016).

Besides, exosomes protein markers including tetraspanin family proteins (CD63, CD9, CD81, and CD82), members of ESCRT complex (TSG101, Alix), and heat shock proteins (HSP60, HSP70, HSPA5, CCT2, and HSP90) (Théry, Ostrowski, and Segura 2009; Simpson et al. 2009; Yoshioka et al. 2013; Fernanda T. Borges et al. 2013; Yokoi, Yoshioka, and Ochiya 2015; Ciardiello et al. 2016; Ha, Yang, and Nadithe 2016). While, microvesicles membrane are enriched with cholesterol, diacylglycerol, and phosphatidylserine (Colombo, Raposo, and Théry 2014); and integrins, selectins, and

CD40 are the main protein markers for this category of EVs (Colombo, Raposo, and Théry 2014).

Furthermore, apoptotic bodies are distinguished from the other two major EV groups by the presence of fragmented DNA and cell organelles from their host cell (Mathivanan, Ji, and Simpson 2010; Akers et al. 2013; Boukouris and Mathivanan 2015). Moreover, apoptotic bodies have exposed phosphatidylserine on their membranes, and their major protein markers include histones, thrombospondin (TSP), and complement protein C3b (Théry et al. 2001).

1.3. EVs as modulators of the tumor microenvironment

Tumor-derived EVs have been recently emerged as putative biological mediators in cancer (Rak and Guha 2012). EVs are highly specialized molecules in cellular communication, as they carry several oncogenic proteins, nucleic acids, and signaling molecules that can be transferred horizontally to the target cells and modulate the tumor microenvironment (TME) for supporting tumor growth, invasion, and metastasis (Higginbotham et al. 2011; Rak and Guha 2012; Tovar-Camargo, Toden, and Goel 2016). The role of EVs in cancer progression and metastasis is described in detail below.

The tumor microenvironment does not only consist of cancer cells but also a heterogeneous population of fibroblasts, endothelial cells, immune cells, cytokines, extracellular vesicles, and extracellular matrix, adipocytes, and vasculature (Balkwill, Capasso, and Hagemann 2012). The crosstalk between cancer cells and their surrounding environment plays a pivotal role in tumor development and progression (Balkwill, Capasso, and Hagemann 2012).

Cancer-associated fibroblasts (CAFs) are one of the most important members within the TME that represent the largest proportion of stroma cells by secreting extracellular matrix components (Xing, Saidou, and Watabe 2010). CAFs can promote the tumor invasion and metastasis, via the secretion of many cytokines such as vascular endothelial growth factor A (VEGFA), C-X-C motif chemokine 12 (CXCL12), Interleukin 6 (IL-6), as well as remodeling of the extracellular matrix (ECM) (Alkasalias et al. 2018).

It was reported that ovarian cancer-derived EVs are capable of modulating fibroblast's behavior towards a CAF-like state. The secretome of these CAFs stimulates the surrounding cells to promote the proliferation, motility, and invasion of the tumor and endothelial cells (Giusti et al. 2018). Moreover, it has been shown that transforming growth factor-beta TGF-β1-associated EVs secreted from prostate cancer can trigger the differentiation of fibroblast into a myofibroblast phenotype resembling stromal cells isolated from cancerous prostate tissue; promoting *in vitro* angiogenesis and accelerating *in vivo* tumor growth (Webber et al. 2015).

Abdouh et al. demonstrated that colorectal cancer (CRC) - derived EVs were able to induce the transformation of fibroblasts into colon carcinoma cells *in vitro* (Abdouh et al. 2019). They showed that fibroblasts treated with CRC-derived EVs mediated the transfer of DNA that was actively transcribed in the fibroblasts after the EVs exposure (Abdouh et al. 2019).

The groups also observed that a definite set of miRNA molecules was transferred from the CRC-derived EVs to the fibroblasts; activating cell cycle progression and cell survival pathways.

Furthermore, the injection of CRC-derived EVs in the tail vein of NOD-SCID mice prompted malignant transformation and metastases in the lungs of the mice (Abdouh et al. 2019).

1.4. Fluorescent labeling of EVs

Several methods have been developed to monitor the biogenesis, transmission, distribution, and subcellular localization of EVs, such as lipid-based fluorescence labelings (Yoshimura et al. 2016; Namba et al. 2018), such as the transmembrane protein CD63 fused with a green fluorescent protein (GFP) and red fluorescent protein (RFP) (CD63-GFP/RFP fusion) (Piao, Kim, and Moon 2019; Mikołaj Piotr Zaborowski et al. 2019), and membrane lipid-binding palmitoylation signal-fused fluorescent proteins such as tandem dimer Tomato (tdTomato) or enhanced green fluorescence protein (EGFP) as I abbreviate as palmGFP (palmG) and palmtdTomato (palmT) (Lai et al. 2015).

Protein S-acylation is a lipid modification that enables the covalent attachment of long-chain palmitic fatty acids to thiol groups of cysteine residues through a thioester linkage (Xu 2011; Verpelli et al. 2012). This type of protein modification is commonly known as S-palmitoylation (S-PALM) allows the association of proteins with cellular membranes (Triola, Waldmann, and Hedberg 2012). The fusion of the fluorescent proteins with palmitoylation sequence to the cell membranes, enabling the whole-cell labeling (Zuber, Strittmatter, and Fishman 1989; Zacharias et al. 2002). As EVs are derived from the plasma membrane (Raposo and Stoorvogel 2013), I assumed that tagging the plasma membrane with fluorescent proteins would enable the labeling of multiple EVs types.

1.5. Structure of MMPs

Metalloproteinases (MMPs) constitute a large family of zinc-calcium dependent endopeptidases and they are considered as the main players in ECM remodeling (Berg, Barchuk, and Miksztowicz 2019). Due to their ability to degrade numerous components of ECM, nucleus matrix, and non-ECM proteins, such as adhesion molecules, cytokines, protease inhibitors, and membrane receptors (Berg, Barchuk, and Miksztowicz 2019).

MMPs play crucial roles in wound healing, angiogenesis, tissue remodeling, as well as in pathological processes, including wound healing (Nagaset and Woessner 1999; Ravanti and Kähäri 2000; Visse and Nagase 2003), inflammation (Y, H, and Jr 1987), and cancer (Coussens and Werb 1996; Curran and Murray 1999; Sternlicht and Werb 2001; Kessenbrock, Plaks, and Werb 2010). So far, the MMP family consists of about 28 members that share similarities in their structure, regulation, and function (Berg, Barchuk, and Miksztowicz 2019).

Based on structure and substrate specificity, MMPs can be further divided into six major subfamilies including collagenases, gelatinases, stromelysins, matrilysins, membrane-type MMPs, and other MMPs (Peng et al. 2012). All MMPs have three principal domains; (1) a pro-domain that functions as an intramolecular inhibitor to maintain the enzyme in an inactive state, (2) a catalytic domain that promotes the proteolytic activity, and (3) a hemopexin-like repeat domain (PEX), which determines the substrate specificity (Figure 2) (Radisky and Radisky 2015).

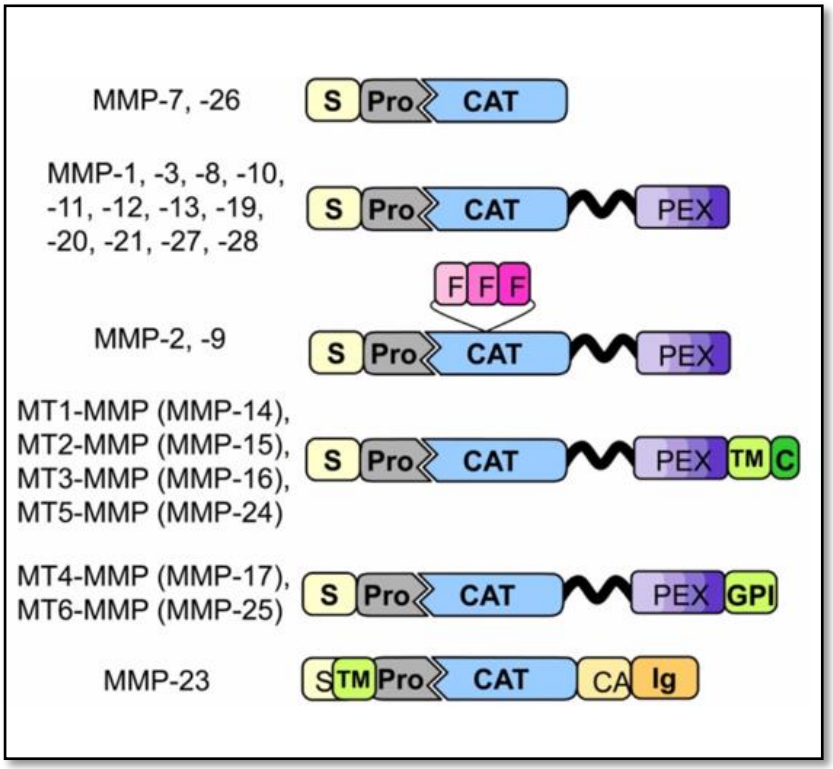

Figure 2. The domain structure of MMPs. S, signal peptide; Pro, pro-peptide; CAT, catalytic domain; F, fibronectin type-II repeats; PEX, hemopexin domain; TM, transmembrane domain; GPI, glycophosphatidylinositol membrane anchor; C, cytoplasmic domain; CA, cysteine array; Ig, immunoglobulin-like domain. Adapted from (Radisky and Radisky 2015).

The PEX domain is found in all MMPs except MMP-7 and MMP-26, thereby they are the smallest MMPs members that having only the pro-peptide and catalytic domains (Murphy et al. 1994; Steffensen, Wallon, and Overall 1995; Shipley et al. 1996; Mikhailova et al. 2012). A more specialized domain including three fibronectin type II repeats, present in MMP-2 and MMP-9 and assist in recognizing elastin and denatured collagen as extracellular matrix

substrates (Murphy et al. 1994; Steffensen, Wallon, and Overall 1995; Shipley et al. 1996; Mikhailova et al. 2012).

Additionally, while most MMPs are soluble extracellular proteins, MMPs-14, -15, -16, and -24 are type I membrane proteins that directly anchored through C-terminal transmembrane domains, MMP-17 and -25 is membrane localized via C-terminal glycophosphatidylinositol (GPI) anchors, and MMP-23 via an N-terminal type II transmembrane domain (Rangaraju et al. 2010). Furthermore, MMP-23 possesses a unique cysteine array that modulates the ion channel activity and an adjacent immunoglobulin-like domain, that similar to the PEX domain of other MMPs (Rangaraju et al. 2010). This array mediates the protein-protein interactions involved in localization or substrate recognition (Rangaraju et al. 2010; Galea et al. 2014).

1.6. Complex roles of MMPs in tumorigenesis

The extracellular matrix serves as a niche for tumor cells to survive and proliferate. On the other hand, it acts as a barrier that suppresses the spreading of tumor cells. Degradation of ECM is one of the first steps in tumor invasion and metastasis (Lu et al. 2011; Venning, Wullkopf, and Erler 2015). ECM remodeling is tightly controlled to maintain tissue homeostasis, integrity, and functions. However, uncontrolled ECM dynamics causes deregulated cell proliferation, invasion, resistance to cell death, and can lead to the development of congenital defects and pathological diseases such as tissue fibrosis and cancer. Moreover, the ECM can act as a barrier against the immune cells or the anticancer drugs, e.g., blocking the penetration of immune cells into the tumor, or creating a high

interstitial fluid pressure (IFP) to prevent the drugs perfusion, thus facilitating cancer immune-escaping and chemoresistance (Lu et al. 2011; Venning, Wullkopf, and Erler 2015).

MMPs were found to promote cell invasion and motility by pericellular ECM degradation. For instance, the expression and activity MMP-2 and MMP-9 are strongly upregulated in human cancers and correlated with the tumor stage, metastasis, and poor prognosis (Lubbe et al. 2006). Besides, MT1-MMP, plays a crucial role in invasion and metastasis, by activating proMMP-2 and directing the cleavage of collagen types I, II, and III (Poincioux, Lizárraga, and Chavrier 2009).

Degradation of the ECM structures by MMPs not only breaks the barrier that prevents the metastatic spread of tumor cells but also produces bioactive molecules that foster tumor growth, proliferation, invasion, and metastasis. For example, cleavage of laminin-5 by MMP-2 and MT1-MMP generates epidermal growth factor EGF-like motifs containing fragments that trigger the epidermal growth factor receptor (EGFR) signaling and other larger fragments that engage the integrin signaling, thereby inducing the tumor cell migration (Koshikawa et al. 2005; Sadowski et al. 2005).

Additionally, osteopontin cleavage by MMP-9 produces a 5-kDa fragment that facilitates tumor cell invasion (Takafuji et al. 2007). What is more, MMP-7 and MMP-9 have been shown to cleave insulin-like growth factor-binding protein (IGFBP), as a result, enhancing the insulin-like growth factor (IGF) bioavailability and activation of insulin-like growth factor receptor (IGFR) signaling (Mañes et al. 1999; 1997; Rorive et al. 2008).

Another study has reported that MT1-MMP cleaves heparin-binding EGF-like growth factor (HB-EGF) and removes the 20 amino acids from the amino (NH2)-terminal region, that are necessary for heparin-binding. The truncated HB-EGF form was found to stimulate the EGFR/ERBB signaling (Rorive et al. 2008; Koshikawa et al. 2010). Moreover, MT1-MMP degrades the protein-tyrosine kinase-7 (PTK7), an inhibitor of cell invasion, thus stimulating cell invasion and migration (Golubkov et al. 2010).

MMPs are capable of modulating cancer progression by promoting invasion, metastasis, and angiogenesis. Both tumor cells and neighboring stromal cells can secret MMPs which degrade the physical barriers and facilitate cancer cells angiogenesis as well as invasion and metastasis (Gialeli, Theocharis, and Karamanos 2011)**.**

Furthermore, MMPs support tumor growth and angiogenesis via increasing the availability of signaling molecules, such as growth factors and cytokines, by liberating them from the ECM (IGF, bFGF, and VEGF) or by increasing their shedding by from the cell surface (EGF, TGF-α, HB-EGF). Besides, MMPs induce angiogenic switch through the downregulation of angiogenic inhibitors and upregulation of angiogenic stimulators factors. Moreover, MMPs can modulate the cell-cell interactions and provoke the ECM through the processing of E-cadherin and integrins, respectively, thereby, increasing cell migration (Figure 3) (Gialeli, Theocharis, and Karamanos 2011).

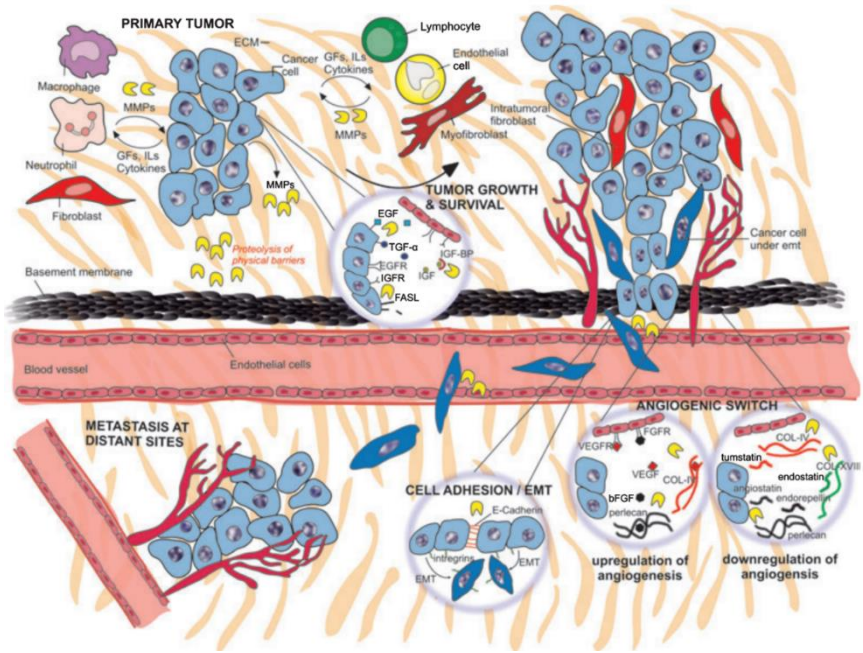

Figure 3. The Pivotal role of MMPs in cancer progression (Gialeli, Theocharis, and Karamanos 2011).

1.7. MMPs in EVs

Several studies have reported that several MMP family members were packaged in EVs from body fluids or various types of cell lines (Dolo et al. 1999; Taraboletti et al. 2002; Belhocine et al. 2010; Shimoda and Khokha 2013; Reiner et al. 2017; Okusha et al. 2020). For instance, prostate cancer-derived oncosomes were shown to contain bioactive MMP2, MMP9 molecules that are involved in local invasion, and correlated with tumor progression (Di Vizio et al. 2012). Another study revealed that vesicles shed from the cultured human umbilical vein endothelial cells are containing active and proenzyme forms of gelatinases, MMP-2 and MMP-9 as well as the MT1-MMP proenzyme that was located on the external side of

the vesicle membrane, all these proteases initiated the proteolysis necessary for tumor invasion and angiogenesis (Taraboletti et al. 2002). Furthermore, MMP13-containing exosomes were found to facilitate the metastasis of nasopharyngeal cancer cells (an endemic type of head and neck cancer associated with a high rate of cervical lymph node metastasis) through the induction of EMT (You et al. 2015).

Also Hendrix et al. reported that Rab27b-mediated exocytic release of HSP90 exosomes from metastatic breast cancer cells can activate MMP2 resulting in the degradation of ECM components and release of growth factors, promotion of cancer cell invasion (Hendrix et al. 2010). Additionally, San-chez et al. have recently demonstrated that prostate cancer stem cells secreted exosomes that are enriched with miRNAs such as miR-100-5p, miR21-5p, and miR-139-5p. These exosomal miRNA increased the expression of MMP2, MMP9, MMP13, and RANKL, also enhanced the fibroblasts migration, thereby contributing to local invasion and pre-metastatic niche formation (Sánchez et al. 2016).

Moreover, Hiratsuka et al. have shown that MMP9 induced by primary tumors in lung endothelial cells and macrophages significantly promoted the lung metastasis, the induction of MMP9 was dependent on the tyrosine kinase VEGFR-1 (Hiratsuka et al. 2002). Blocking of the MMP9 induction via deletion of either VEGFR-1TK or MMP9 markedly diminished the lung metastasis in mice models (Hiratsuka et al. 2002).

1.8. The two-dimensional and three- dimensional culture systems

The two-dimensional (2D) cell culture system has been frequently used for cancer research and drug screening (Yoshii et al. 2011). In conventional 2D culture systems, cells are cultured as monolayers on flat surfaces of plates which allow each cell to access the same amount of growth factors and nutrients present in the medium, resulting in homogenous growth and proliferation (Edmondson et al. 2014). Besides, the strong physical interaction present between cells and 2D culture substrates resulted in alteration in the tumor cell behaviors that differ from those of tumors growing *in vivo* (Yoshii et al. 2011). Thus, the 2D culture model fails to correctly mimic the proper tissue architecture and complex microenvironment *in vivo* (Lv et al. 2017).

To overcome the limitations of the 2D culture system, a three-dimensional (3D) cell culture model (aka a spheroid or organoid culture) have been developed to better mimic *in vivo* tissue microenvironments (Lv et al. 2017; Duval et al. 2017). The 3D culture model maintains the interactions between cells and their ECM, create gradient access of oxygen and nutrient, and buildup a combination of tissue-specific scaffolding cells (Griffith and Swartz 2006).

Similar to human cancers, proliferating, quiescent, and dying cells are coexisting in normoxic, hypoxic, or necrotic zones within tumor organoids (Hirschhaeuser et al. 2010; Eguchi et al. 2018; Namba et al. 2018). Thus, the 3D tumor models reflect more closely the *in vivo* human tumors, which prompted us to define tumor organoids as “tumoroids”. Among several methodologies of tumoroid models, we have adopted gel-free tumoroid models cultured on

NanoCulture Plates (NCP) and ultra-low attachment (ULA) plates (Arai et al. 2016; Eguchi et al. 2018; Namba et al. 2018; Sogawa et al. 2019; 2020).

A great advantage of the gel-free tumoroid model is the collectability of the secretome including EVs from their culture supernatants. NCP is a nanopatterned gel-free scaffold for 3D cell culture (Elsayed and Merkel 2014). The mogul field structure on NCPs restricts cells to sprawl on the base and enable tumor cells to migrate from a scaffold to another scaffold more actively than cells cultured on the 2D plate.

The increased migration and lesser attachment of cancer cells on the NCPs enable tumor cells to form 3D tumoroids (Arai et al. 2016; Eguchi et al. 2018; Namba et al. 2018; Sogawa et al. 2019; 2020). ULA plates have been also useful for the collection of secretome including EVs. Cells do not rapidly migrate on ULA plates compared to NCPs. We have examined a few types of culture media such as serum-containing media versus serum-free stemness-enhancing media in combination with the 3D culture systems. *In vitro* culture of tumoroids in such a 3D nano-environment combined with a defined stem cell medium enabled the cells to grow slowly and form large organoids that expressed multiple stem cell markers and intercellular adhesion molecules (Eguchi et al. 2018; Namba et al. 2018).

2. Aim and objective

Here, I explored (i) the tumorigenic role of MMP3 on the *in vitro* tumoroid formation under the 3D culture system and on their EVs integrity, (ii) whether MMP3-rich or MMP3-null EVs could alter tumoroid formation, and examined (iii) the EVs-mediated molecular transfer of MMP3 into the MMP3-KO tumoroids under the 3D culture system.

3. Materials and methods

3.1. Cells

A rapidly metastatic murine cancer cell line LuM1 (Sakata et al. 1996; Namba et al. 2018; Sogawa et al. 2020) and MMP3-KO cells line (Okusha et al. 2020) were maintained in RPMI-1640 with 10% fetal bovine serum (FBS) and penicillin, streptomycin, and amphotericin B. MMP3-KO cells were established using the CRISPR/Cas9 system from the LuM1 cell line (Okusha et al. 2020). Briefly, Cas9 protein and guide RNA that targets *Mmp3* exon 1 were co-transfected into LuM1 and stable MMP3-KO clones with frame-shifting deletion were obtained.

3.2. Tumoroid culture

Tumoroids were formed in the 3D culture systems using NanoCulture Plate (NCP) (Medical & Biological Laboratories, Nagoya, Japan) or ultra-low attachment (ULA) culture plates/dishes (Greiner, Kremsmunster, Austria) within mTeSR1 stem-cell medium (Stemcell Technologies, Vancouver, Canada) or the above-mentioned serum-containing medium as described previously (Eguchi et al. 2018; Namba et al. 2018; Sogawa et al. 2019; 2020).

For quantification of tumoroids size and number, cells were seeded in a 96 well NCP for 14 days at a concentration of 5.0×10^3 cells in 200 μL mTeSR1 or RPMI-1640 media with 10% FBS. Tumoroid maturation was monitored every day and photographed using the Floid cell imaging station (Thermo Fisher, Waltham, MA, USA) from day 1 until day 7 and a BZ-X microscope (Keyence, Osaka, Japan) starting from day 10 until the end of the experiment

day 14. The tumoroid size was measured using Image J software (NIH, Bethesda, MD, USA).

3.3. 2D re-seeding assay

Tumoroids were cultured in the 3D and stem-cell medium condition for 14 days and detached by trypsin/EDTA. The detached cells were re-seeded in a 24-well 2D culture plate at a concentration of 1.5×10^4 cells/well in RPMI-1640 with 10% FBS. The cell images were taken by using the Floid cell imaging station (Thermo Fisher, Waltham, MA, USA) on days 2, 4, 6, and 7 after the seeding.

3.4. Preparation of EVs and conditioned media

Tumoroid-derived EVs were used for tumoroid formation assays. Otherwise, 2D cultured cells-derived CM was used for 2D experiments. EVs were prepared from culture supernatants of tumoroids using a modified polymer-based precipitation method (Fujiwara et al. 2018; Ono et al. 2018; Eguchi et al. 2020). Briefly, cells were seeded on a 10-cm ULA dish at a density of 1.0×10^6 cells/8 mL mTeSR1 medium and cultured for 6 days. The formed tumoroids were washed with PBS (-), and then further cultured in serum-free medium (4 mL per dish) for 2 days. Cell culture supernatant was collected and centrifuged at 2,000 × *g* for 30 min at 4°C to remove detached cells. The supernatant was then centrifuged at 10,000 × *g* for 30 min at 4°C to remove cell debris. The supernatant (8 mL) was concentrated to less than 1 mL by using an Amicon Ultra-15 Centrifugal Filter Devices for M.W. 100k (Merck Millipore, Burlington, MA). The concentrate was applied to the Total EVs Isolation System (Thermo Fisher, Waltham, MA, USA). The pass-

through was concentrated using an ultrafiltration device for molecular weight 10 kD and used as a non-EV fraction. The EV fraction was suspended in 100 µL PBS (-) and used 3D-tumoroid-EVs. Protein concentration was measured using a micro BCA protein assay kit (Thermo Fisher, Waltham, MA, USA).

For immunofluorescence in the 2D culture system, culture supernatants were collected from serum-free media of 2D-cultured donor cells during the exponential growth phase (70% confluence). The culture supernatants were centrifuged at 2,000 x *g* for 15 min to get rid of cells and debris, followed by diluting in a ratio 1:1 with a fresh culture medium. The CM was stored at -80°C. Recipient cells were treated with the CM for 48 h.

3.5. Transmission electron microscopy

As described previously (Eguchi et al. 2018; 2020), a 400-mesh copper grid coated with formvar/carbon films was hydrophilically treated. The EVs suspension (5-10 µL) was placed on Parafilm, and the grid was visualized at 5,000, 10,000, or 20,000 times magnification with an H-7650 transmission electron microscope (TEM) (Hitachi, Tokyo, Japan) at the Central Research Laboratory, Okayama University Medical School.

3.6. Particle diameter distribution

As described previously (Fujiwara et al. 2018; Eguchi et al. 2020), 40 µL of EV fraction within PBS (-) was used. Particle diameters of the EV fractions in a range between 0 and 6,000 nano-diameters were analyzed in Zetasizer nano ZSP (Malvern Panalytical, Malvern, UK).

3.7. Western blotting

Western blotting was performed as described (Ono et al. 2018; Eguchi et al. 2020). Cells were cultured for 6 days on a 6 well ULA plate at a density of 3.0 x 10^5 cells/3 mL mTeSR1 medium in a well. Cells were further cultured in serum-free media for 2 days. On day 8, the supernatants and tumoroids were collected, centrifuged at 2000 x *g*, 4˚C for 5 min. The supernatants were used for EV preparations as mentioned above.

To prepare whole cell lysate (WCL), tumoroids were lysed in a RIPA buffer (1% NP-40, 0.1% SDS, and 0.5% deoxycholate, and EDTA-free protease inhibitor cocktail in PBS) using 25-gauge syringes. The cell lysate was incubated for 30 min on ice and then centrifuged at 12,000 *g* for 20 min at 4˚C. The preparation method of EV and non-EV fraction was described above. The supernatant was used as WCL. The same protein amounts for each lane were subjected to sodium dodecyl sulfate-polyacrylamide gel electrophoresis (SDS-PAGE), followed by transfer to a polyvinylidene fluoride (PVDF) membrane using a semi-dry transfer system.

The membranes were blocked in 5% skim milk in Tris-buffered saline containing 0.05% Tween 20 for 60 min at room temperature (RT) and then incubated overnight with rabbit monoclonal antibodies; anti-MMP3 (EP1186Y, ab52915, Abcam, Cambridge, UK) or anti-CD9 (EPR2949, ab92726, Abcam, Cambridge, UK) or anti-CD63 (EXOAB-CD63A-1, System Biosciences). For CD63, blocking was performed in 10% overnight and the primary antibody was reacted for 2 days. The membranes were incubated with horseradish peroxidase (HRP)-conjugated secondary antibodies. For GAPDH, the HRP-conjugated anti-GAPDH mouse monoclonal antibody (HRP-60004,

Proteintech, Rosemont, IL, USA) was used. For Actin, anti-Actin rabbit antibody (A2066, Sigma Aldrich, St. Louis, MO, USA) was utilized. Blots were visualized with the ECL substrate (Merck Millipore, Burlington, MA, USA).

3.8. Coomassie blue staining (CBS)

Protein samples (1 µg each) were loaded on the SDS-PAGE. After the electrophoresis run, the gel was stained with Coomassie Brilliant Blue R-250 solution (1610436, Bio-Rad, Hercules, CA, USA) for 30 min with gentle agitation followed by washing with the destaining solution (50% methanol, 10% glacial acetic acid) for 2 h until the background became less dark.

3.9. EV-driven *in vitro* tumorigenesis

MMP3-KO cells were seeded at 5.0 x 103 cells/200 µL mTeSR1 medium in a well of 96-well NCP. After two days, EVs derived from 3D-tumoroids (LuM1 or MMP3-KO) were added to MMP3-null tumoroids at a final concentration of 5 µg/mL. Then the plate was centrifuged at 1,800 × g for 1 h at 4˚C to increase the internalization of EVs into the tumoroids (Lai et al. 2015). The MMP3-KO tumoroids maturation was monitored over 14 days using a microscope FSX100 (Olympus Life Science, Tokyo, Japan). Then tumoroid size was measured using Image J.

3. 10. Palm fluorescent cells

The lentiviral reporter constructs of CSCW-palmitoylation signal-tandem dimer Tomato (palmT) and CSCW-palmitoylation signal-EGFP (palmG) were kindly gifted from Dr. Charles P. Lai (Lai

et al. 2015). For virus production, HEK293T cells at 70-80% confluence were transfected with PalmT or PalmG constructs, psPAX2 packaging plasmid, and pMD2.G envelope plasmid using PEI max (Polysciences).

LuM1 or MMP3-KO cells were infected by using the spinfection method with the viral solution. Infected/transduced stable cells were selected using puromycin. Isolation of single clones was carried out by limiting dilution method. We established palmtdTomato-expressed LuM1 cells (designated LuM1/palmT), palmGFP-expressed LuM1 cells (designated LuM1/palmG), palmGFP-expressed MMP3-KO cells (designated MMP3-KO/palmT), and palmGFP-expressed MMP3-KO cells (designated MMP3-KO/palmG).To confirm fluorescent labeling, the palm fluorescent cells were seeded on a type I collagen-coated coverslip in a 24-well plate at a density of 1×10^4 cells/well in a serum-containing culture media and cultured for 48 h.

3.11. EVs exchange assay

Two different colored fluorescent cells (LuM1/palmG and LuM1/palmT cells) were used as donor cells or recipient cells with each other in the 2D culture system. The donor cells were seeded at 1×10^6 cells in a 60 cm dish and cultured overnight in a serum-containing culture media. The grown cells of 70-80% confluence were washed twice with PBS, then the culture media was replaced with a serum-free medium and cultured for a further 2 days. The culture supernatant was collected and centrifuged at $2{,}000 \times g$ for 15 min at 4°C to remove detached cells and the supernatants were diluted in a ratio 1:1 with a fresh culture medium and used as CM. Recipient cells were seeded on a type I collagen-coated coverslip inserted in a

24-well plate at a density of 1×10^4 cells/well and cultured for 24 h in a serum-containing culture media. The recipient cells were treated by donor cells-derived CM for 48 h. For coculturing, recipient MMP3-KO cells were seeded on coverslips. LuM1-donor cells (1×10^4 cells/well) were seeded on a culture insert with a 0.45-μm pore (Greiner, Kremsmunster, Austria) in a 24 well plate. The insert with donor cells was placed on the well containing the recipient cells and cocultured for 48 h.

3.12. 2D confocal laser-scanning microscopy

Cells were fixed in 4% paraformaldehyde (PFA) for 10 min at RT and permeabilized with 0.5% Tween-20 for 10 min. For blocking the non-specific reaction of primary antibodies, cells were blocked in 10% normal goat serum solution (Dako, Tokyo, Japan) for 30 min, then incubated overnight at 4℃ with rabbit anti-MMP3 antibody (EP1186Y, ab52915, Abcam, Cambridge, UK) or rabbit anti-CD9 antibody (EPR2949, ab92726, Abcam, Cambridge, UK), for overnight at 4˚C and subsequently with a secondary antibody, goat anti-rabbit IgG Alexa Fluor 488 (A-11034, Thermo Fisher, Waltham, MA, USA) for 1 h at RT.

As a negative control, the same protocol was performed without primary antibody staining. Washes after antibody reactions were done with PBS, three times for 3 min each, on a shaker at RT. The mounting and DNA staining was performed by using Immunoselect Antifading Mounting Medium DAPI (SCR-038448, Dianova, Germany). Fluorescent images were taken using a confocal laser scanning microscopy LSM780 (Carl Zeiss, Oberkochen, Germany) at Central Research Laboratory, Okayama University Medical School.

3.13. Immunofluorescence of tumoroids

For tumoroid formation, cells were cultured for 6 days at a density of 3.0 x 10^5/3 mL mTeSR1 in a well of a 6-well ULA plate. Then tumoroids were treated with PBS, the 3D-tumoroid LuM1-EVs at a final concentration of 5 µg/mL or the 3D-tumoroid LuM1-CM (diluted 1:1 with fresh mTeSR1) for 24 h. Then the plate was centrifuged at 1,800 × *g* for 1 h at 4˚C to increase the internalization of EVs into the tumoroids (Lai et al. 2015). Tumoroids were washed with PBS and fixed in 4% PFA for 10 min.

Tumoroids were additionally washed with PBS for 5 min 3 times and embedded in paraffin. Tumoroids sections (5 µm thickness) were deparaffinized and hydrated through xylenes and graded alcohol series. Antigen retrieval was performed by heating the specimens in Tris/EDTA buffer, pH 9.0 (Dako target retrieval solution S2367, DAKO, Carpenteria, CA) using a microwave for 3 min for CD9 or by autoclaving in 0.01M citrate buffer pH 6.0 (sodium citrate dihydrate, citric acid; Sigma Aldrich, USA) in a pressure cooker for 8 min for MMP3 and Ki-67.

Sections were treated with blocking solution (Dako) for 30 min at RT, then incubated with primary antibodies; rabbit anti-CD9 (EPR2949, ab92726, Abcam, Cambridge, UK), rabbit anti-MMP3 (EP1186Y, ab52915, Abcam, Cambridge, UK), or rat anti-Ki-67 antibody (TEC-3, M7249, Dako); individually at 4°C overnight. Then, sections were subsequently stained with a secondary antibody goat anti-rabbit IgG, Alexa Fluor 488 (A-11034, Thermo Fisher, Waltham, MA, USA) for 1 h at RT. Then samples were counterstained with 1 mg/mL of DAPI (Dojindo Laboratories, Kumamoto, Japan). Fluorescent images were taken using a confocal

laser scanning microscopy LSM780 (Carl Zeiss, Oberkochen, Germany) at Central Research Laboratory, Okayama University Medical School.

For IHC staining of Ki67, a biotinylated secondary antibody was applied for 30 min (Vector Lab, Burlingame, CA) and the color was developed with 3, 3'-diaminobenzidine (DAB) (Histofine DAB substrate; Nichirei, Tokyo, Japan). Then, samples were counterstained with Myer's hematoxylin and images were taken using an optical microscope BX53 (Olympus).

To calculate the Ki-67 labeling index (%), we counted approximately 100 Ki67-positive cells were counted in random five fields under the 40× objective. Areas with severe necrosis were avoided. The Ki-67 labeling index (%) was calculated by dividing the total Ki-67 positive cells by the total numbers of cells multiplied by 100. The total tumoroid areas, as well as the area of necrotic regions, were measured using Image J. The percentage of necrosis was calculated by dividing the total necrotic area by the total tumoroid area.

3.14. Hematoxylin and eosin staining

For tumoroid formation, LuM1 or MMP3-KO cells were cultured for 8 days on 6 well ULA plates at a density of 3.0 x 10^5/3 mL mTeSR1/well. Then tumoroids were washed with PBS, fixed in 4% PFA for 10 min, and embedded in paraffin. Tumoroids sections (5 µm thickness) were deparaffinized in a series of xylene for 15 min, rehydrated in graded ethanol solutions, and washed well in distilled water. Then sections were incubated in Harris hematoxylin solution for 10 min and rinsed in tap water until the water was colorless.

Finally, after sequential treatment with hydrogen chloride and 80% ethanol solution, sections were incubated in eosin for 7 min.

3.15. Tracing EV-uptake *in vitro*

Ten micrograms of tumoroid-derived EVs were incubated with 0.25 µM BODIPY TR Ceramide (Thermo Fisher, Waltham, MA, USA) for 20 min at 37°C. Excessive BODIPY TR Ceramide was removed with Exosome Spin Columns (MW 3000) (Thermo Fisher, Waltham, MA, USA) (Namba et al. 2018). Cells were seeded at a concentration of 5.0 x 10^3 cells/200 µL mTeSR1 in a well of 96-well NCP. The next day, EVs were added at a final concentration of 5 µg/mL. The EVs-uptake was monitored over 24 h using the ArrayScan High Content Screening (HCS) system (Thermo Fisher, Waltham, MA, USA). The fluorescence intensity of each cell was determined using a filter set (485/594) for (GFP/ BODIPY TR). The average fluorescence intensity of the PBS treatment group at time point 0 h was evaluated as background and subtracted from raw values.

3.16. Statistical analysis

Statistical significance was calculated using GraphPad Prism and Microsoft Excel. The difference between the sets of data was analyzed using ANOVA Tukey's multiple comparisons test and all data are expressed as the mean ± standard deviation unless otherwise indicated.

4. Results

4.1. MMP3 knockout reduces the release of CD9 and CD63 within extracellular vesicles

To explore the role of MMP3 on cellular communication in cancer, our research group has generated MMP3-KO cells by the CRISPR/Cas9 genome editing system from a rapidly metastatic murine cancer cell line LuM1 with a parental cancer cell line Colon26 (aka CT26) (Okusha et al. 2020). The release of EV proteins from MMP3-KO-tumoroids tended to decrease compared to LuM1-tumoroids (Figure 4A-D). However, there was no statistically significant difference in the protein concentration of the whole cell lysate (WCL) between LuM1 and MMP3-KO-tumoroids.

MMP3 was markedly detected in the cellular, non-EV, and EV fractions of the LuM1, while the complete loss of MMP3 was confirmed in MMP3-knockout LuM1 cells, non-EV (including soluble proteins), and EV fractions (Figure 4E, top row; Figure S1A), suggesting a successful knockout of the Mmp3 gene.

Next, I examined CD9 (a category-1 EV marker protein) expression pattern. Interestingly, the CD9 content was significantly down-regulated in both cellular and EV fractions of the MMP3-null cells compared to their counterpart (Figure 4E, second and third rows; Figure S1B). Moreover, CD63 was reduced in the EV fraction of the MMP3-null cells (Figure 4E, fourth and fifth rows; Figure S1C). Recently, we have shown that GAPDH and β-actin were released in the EV and non-EV soluble fractions upon membrane-damaging cell stress (Eguchi et al. 2020). Therefore, I examined the expression

levels of β-actin and GAPDH not only as a loading control but also to investigate whether they were released within EVs or non-EV soluble proteins. Our results revealed that both β-actin and GAPDH were detected in the EVs derived from both cell lines, but not in the non-EV fractions (Figure 4E, bottom lane; Figure S1D, E; Figure S2A). Notably, β-actin levels were considered as a loading control for WCL and EV fractions, whereas GAPDH was not (Figure S1D, E). Furthermore, the SDS-polyacrylamide gel was stained with Coomassie brilliant blue (CBB) after the electrophoretic separation (Figure S2B).

These findings demonstrate that MMP3 controls the secretion of CD9/CD63-contained EVs.

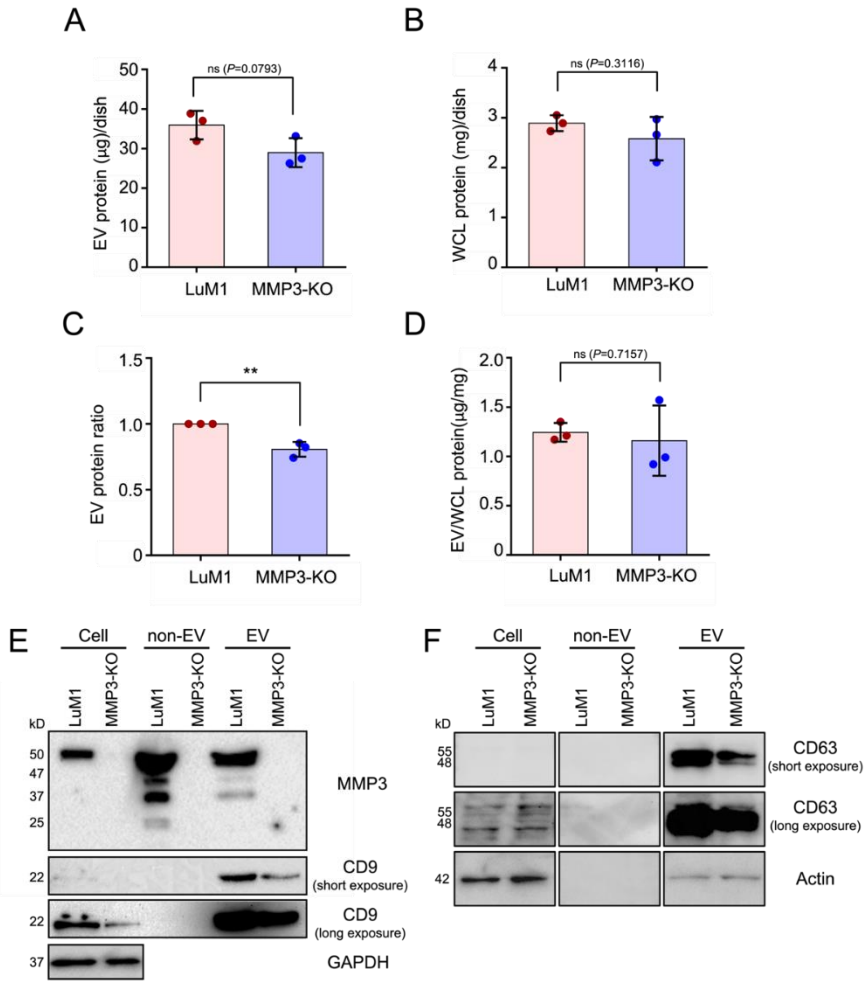

Figure 4. MMP3 knockout reduces the release of CD9 and CD63 within extracellular vesicles. Tumoroids were formed in 10-cm ultra-low attachment (ULA) plates for 6 days. Extracellular vesicle (EV) and non-EV fractions were collected from the culture supernatants. (**A**, **B**) The total protein concentration in the (**A**) EV and (**B**) whole cell lysate (WCL) fractions of LuM1-tumoroids and MMP3-KO tumoroids. (**C**) Relative EV protein ratio comparing two cell lines. (**D**) EV protein concentration per the WCL proteins. ** $p < 0.01$; ns, not significant. (**E**) Western blotting showing MMP3, CD9, CD63, and β-actin in tumoroids, non-EV, and EV fractions. The 54-kD

bands indicate the full-length MMP3, the 47-kD bands represent the active form consists of the catalytic, hinge, and PEX domains, the 37-kD represents the catalytic domain, and the 25-kD shows the PEX domain of MMP3. The expression level of β-actin was examined as a loading control as well as to check if it was released from cells. The protein amounts loaded from WCL and EV fractions were 10 μg per lane, while 5 μg per lane was loaded from the non-EV fractions. The experiments were repeated twice. For full images of Western blotting, see Figure S1.

4.2. MMP3 knockout impacts physical integrities of extracellular vesicles

Further, I examined the morphology and size of EVs secreted from "tumoroids" by transmission electron microscopy (TEM) and Zetasizer, respectively. Both LuM1- and MMP3-KO tumoroids released two types of EVs small EVs (s-EVs) ranged approximately 50-200 nm and large EVs (L-EVs) more broadly ranged between 200 and 1000 nm (Figure 5A, B, Table 1). According to their size, the s-EVs were supposed to be exosomes, while the L-EVs were supposed to be microvesicles.

Meanwhile, crescent moon-like shaped and broken EVs were particularly seen in the MMP3-KO EV fraction released by MMP3-KO tumoroids (Figure 5A, B). Additionally, I observed large aggregates (500-800 nm) of EVs derived from MMP3-KO compared to their counterparts (Figure 5C).

Particle diameter distribution analysis using Zetasizer revealed that the size of both s-EVs (peaked at 84 nm) and L-EVs (peaked at 465 nm) released from MMP3-KO tumoroids were smaller than those (peaked at 119 nm and 561 nm, respectively) of LuM1 tumoroids

(Figure 5D, E). The small particles detected at 5-10 nm in the LuM1-EV fraction might be damaged membrane vesicles or lipoprotein particles e.g. HDL (5–12 nm) which have similar size ranges as EVs (Schumaker 1994).

These findings demonstrate that MMP3 is important for maintaining the physical integrities of EVs, and the loss of MMP3 resulted in disorganizing the EVs structures.

Table 1. Comparison of particle size distributions between LuM1-EVs and MMP3-KO-EVs.

	LuM1-EV				MMP3-KO-EV		
Peak	Diameter (nm)	Intensity (%)	Width (nm)	Peak	Diameter (nm)	Intensity (%)	Width (nm)
1	561.4	48.6	164.9	1	464.9	76.6	155.3
2	119.3	38.3	31.8	2	83.9	20.2	20.4
3	8.0	6.8	1.53	3	5374	3.2	326.1

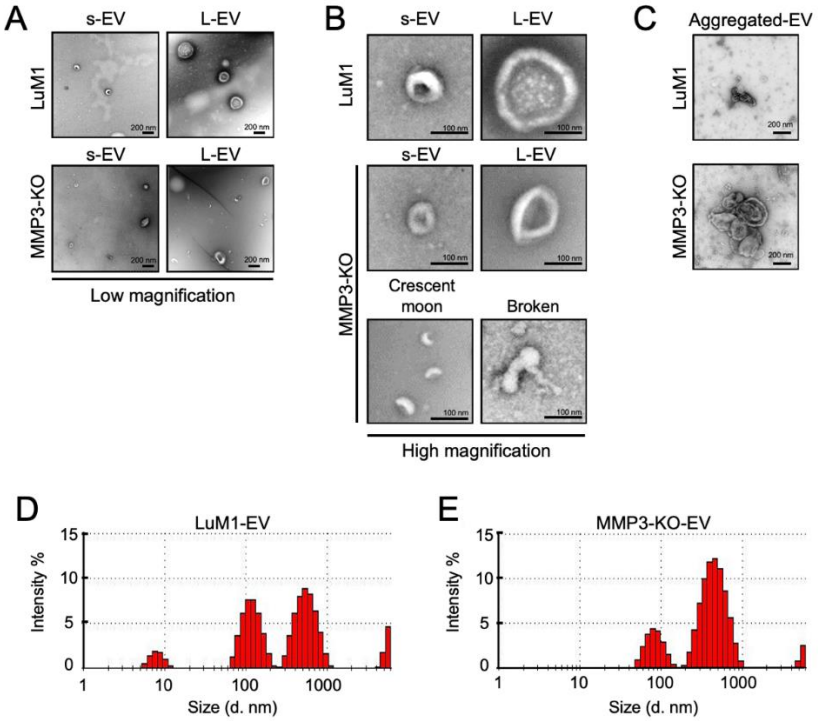

Figure 5. MMP3 knockout impacts the physical integrities of extracellular vesicles. (**A-C**) TEM images of EV fractions derived from the LuM1 and MMP3-KO tumoroids. at **(A)** low magnification, **(B)** high magnification, and of **(C)** aggregated EVs. s-EVs, small EVs; L-EVs, large EVs. Scale bars, 200 nm (in low magnification), and 100 nm (in high magnification). **(D, E)** Representative histograms showing the particle diameter distributions of EVs derived from **(D)** LuM1 tumoroids and **(E)** MMP3-KO tumoroids. The experiments were repeated twice.

4.3 Loss of the *Mmp3* gene reduces the *in vitro* tumorigenicity

Next, I examined the consequences of *Mmp3* loss on the *in vitro* tumoroid formation. The LuM1 and MMP3-KO cells were cultured in the 3D culture system either under serum-containing or mTeSR1 stemness-enhancing conditions for 14 days. Larger tumoroids were formed in the stemness-enhancing medium compared to smaller tumoroids seen in the serum-containing medium (Figure 6A-G).

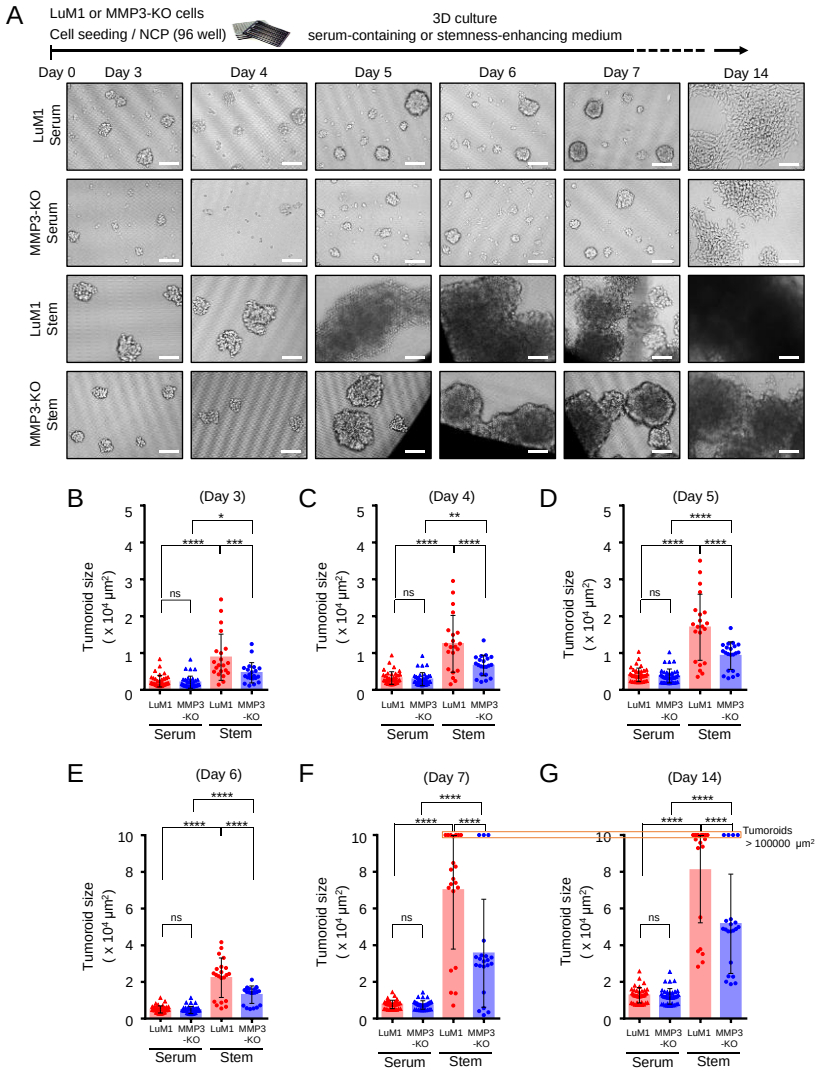

Figure 6. The loss of the *Mmp3* gene reduces the *in vitro* tumorigenicity. Tumoroids were formed in the NanoCulture Plate (NCP)-based 3D culture with a serum-containing or stemness-enhancing medium. (A) Representative images of the LuM1 and MMP3-KO tumoroids. The upper panel shows the experimental design. (B–G) Tumoroid size quantification on (B) day 3, (C) day 4, (D) day 5, (E) day 6, (F) day 7, and (G) day 14 of the tumoroid growth periods. N = 39 (LuM1 serum, MMP3-KO serum), n = 21 (LuM1 stem, MMP3-KO stem). * $p < 0.05$, ** $p < 0.01$, *** $p < 0.001$, **** $p < 0.0001$; ns, not significant. The alternative graphs of Figure 3F, G

with tumoroid plotting larger than 100,000 μm^2 are shown in Figure S3. The experiments were repeated twice.

A highly significant difference in the tumoroid size between LuM1 and MMP3-null cells was observed under the stemness-enhancing culture conditions from day 3 until day 14 (Figure 6A–G; Figure S3). The size of MMP3-null tumoroids was significantly smaller compared to LuM1 tumoroids (Figure 6B, G; Figure S3).

Subsequently, I asked whether MMP3-KO and LuM1 cells were able to grow if they reseeded under the 2D culture conditions or not. I trypsinized tumoroids and reseeded under the 2D culture condition. Both cell types proliferated and reached confluency by day 7. More interestingly, LuM1 cells were able to grow into tumoroids even under the 2D culture condition, whereas MMP3-null cells were not (Figure 7).

These data suggest that the stemness-enhancing medium promotes the tumorigenic aggregation of tumor cells, whereas the serum-containing medium stimulates the cellular differentiation and decreasing the fusion of tumoroids. Besides, these findings indicate that loss of MMP3 has a great significance on inhibiting the tumoroid formation *in vitro*.

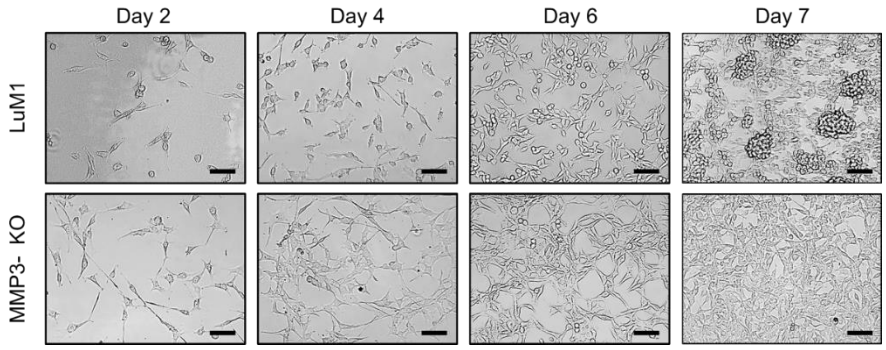

Figure 7. Representative images of re-cultured LuM1 and MMP3-KO cells in 2D culture. Tumoroids on day 14 were trypsinized and re-cultured under the 2D culture condition in serum-containing media. Scale bars, 100 μm. The experiment was repeated twice.

4.4. The addition of MMP3-rich EVs accelerated the *in vitro* tumorigenesis of MMP3-KO cells.

I further investigated whether treating the MMP3-KO tumoroids with LuM1-EVs (MMP3-rich) or MMP3-KO-EVs (MMP3-null) would foster the *in vitro* tumorigenesis under the 3D culture system. A protocol has been shown that seeding the cells first followed by the addition of EVs two days later and centrifuging the plate improves the uptake of EVs into cells (Lai et al. 2015). As a pilot study, I examined this protocol to see the effect of three different concentrations (1.25, 2.5, and 5 μg/mL) of LuM1-EVs on the growth or cytotoxicity in MMP3-KO tumoroids. With this protocol, I found that the addition of 5 μg/mL of EVs significantly promoted the tumoroid growth compared to the lower concentrations of EVs (Figure S4).

I then found that the addition of LuM1-EVs tended to increase the size of tumoroids from the next day of the EVs addition to 12 days later, while the addition of MMP3-KO-EVs might not promote the tumoroid growth (Figure 8A). The growth of MMP3-KO tumoroids following the different treatments was monitored by plotting the average tumoroid size over the time following the different treatments (Figure 8B). The addition of LuM1-derived EVs fostered the tumoroids growth compared to the other two groups.

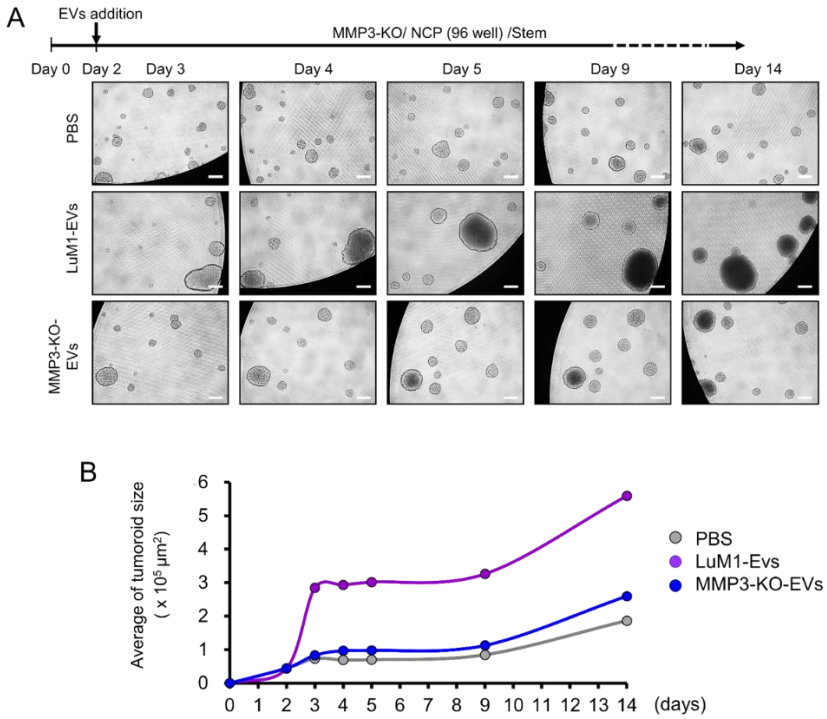

Figure 8. The addition of MMP3-rich EVs accelerated the *in vitro* tumorigenesis of MMP3-KO cells. MMP3-KO tumoroids were treated with PBS, LuM1-EVs, or MMP3-KO-EVs at a final concentration of 5 μg/mL in the NCP-based 3D culture with the stemness-enhancing medium. **(A)** Experimental scheme (top) and representative photomicrographs (bottom) of tumoroid maturation at the indicated timepoints. Scale bar, 100 μm. **(B)** A time plot graph

showing the average size of the MMP3-KO tumoroids following the different treatments over the indicated timepoints. See the next figure for statistical analysis.

Notably, the addition of LuM1-EVs resulted in significant increases in the size of tumoroids from the next day of the EVs addition to 12 days later, while the addition of MMP3-KO-EVs did not have any impact on the tumoroid growth (Figure 9A, B). In parallel, the comparison of the top 20 tumoroid sizes in the three groups revealed that the addition of LuM1-derived EVs significantly potentiated the formation of enlarged tumoroids compared to the other treatments with MMP3-KO-EVs or PBS (Figure 9C, D).

I thus found that that (i) MMP3-high, LuM1-derived EVs augmented the tumor growth *in vitro,* and (ii) the loss of MMP3 in EVs diminished the protumorigenic properties of the EVs.

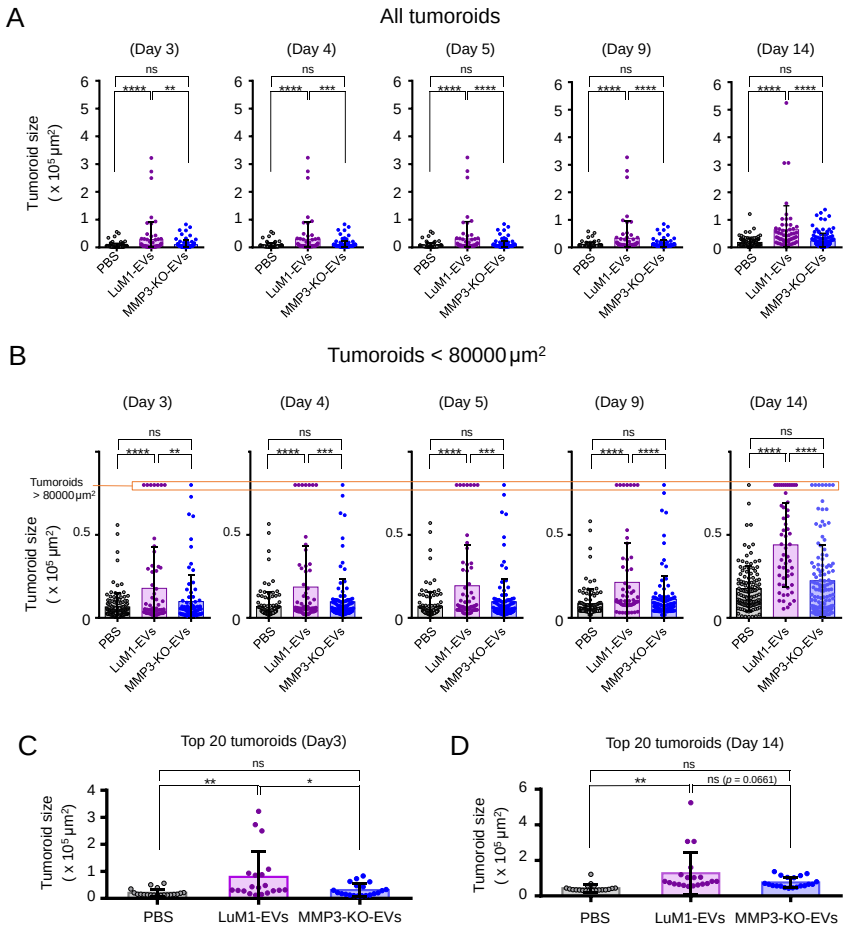

Figure 9. Tumoroid size was altered by the addition of LuM1-EVs versus MMP3-KO-EVs. (A, B) Tumoroid size quantification of **(A)** all tumoroids and **(B)** tumoroids smaller than 80000 µm^2 at the indicated time points of the tumoroid formation. Cell aggregates (>500 µm^2) were considered to be tumoroids. **(B)** Tumoroids larger than 80000 µm^2 were shown on the top of the graph. **(C, D)** Top 20 tumoroids size quantification on **(C)** day 3 and **(D)** day 14. * $p < 0.05$, ** $p < 0.01$, *** $p < 0.001$, **** $p < 0.0001$; ns, not significant; n = 54–130 (number of plots). The experiments were repeated twice.

4.5. Establishment of fluorescent-labeled LuM1 and MMP3-null cells

It has been shown that EVs were derived from the plasma membrane (Colombo, Raposo, and Théry 2014) and could be labeled with palmitoylation signal-tagged fluorescent proteins (Lai et al. 2015). To monitor the tumor EVs-uptake and exchange between cell populations, the plasma membrane of the LuM1 and MMP3-KO cells were labeled with palmitoylation signal-fused fluorescent reporters, namely palmG and palmT, thereby green and red labeled cells were established (Figure 10A, B).

In this EVs exchange assay, if the red/green recipient cells have taken up the green/red-EVs from donor cells, an increase in the green/red fluorescence signals should be observed, whereas, in non-treated cells, no green/red fluorescence signals should be detected. Indeed, the green/red fluorescence was markedly detected in the cells treated with the CM of green/red cells, indicating that EVs were exchanged between the cells (Figure 10C, D).

Additionally, I confirmed the EVs-mediated molecular transfer of MMP3 and CD9 under the 2D culture system by treating MMP3-KO cells with LuM1-CM or by co-culturing with the MMP3 produced by the LuM1 cells in the transwell insert. Interestingly, MMP3 was restored and detected in the cytoplasmic and nuclear regions of MMP3-KO recipient cells after the addition of LuM1-CM or coculturing (Figure 10E).

The CD9 expression level was low in the MMP3-KO cells as shown in Figure 1. However, CD9 was significantly increased in the nuclear and cytoplasmic regions of MMP3-KO recipient cells after the addition of LuM1-CM or coculturing (Figure 10F). *Mmp3* was deleted at the genome level, while *Cd9* was not in the MMP3-KO cells. Therefore, as data interpretation, there were two possibilities including that (i) CD9 was transferred from LuM1-EVs to recipient cells and/or (ii) endogenous CD9 was induced in the recipient cells after the stimulation with LuM1-EVs.

Collectively, these data prove the successful labeling and exchanging of EVs between cell populations. Next, I confirmed the exchange of EVs between the cells. Two different colored fluorescent cells LuM1/palmG (green) and LuM1/palmT (red) cells were treated with each other conditioned media

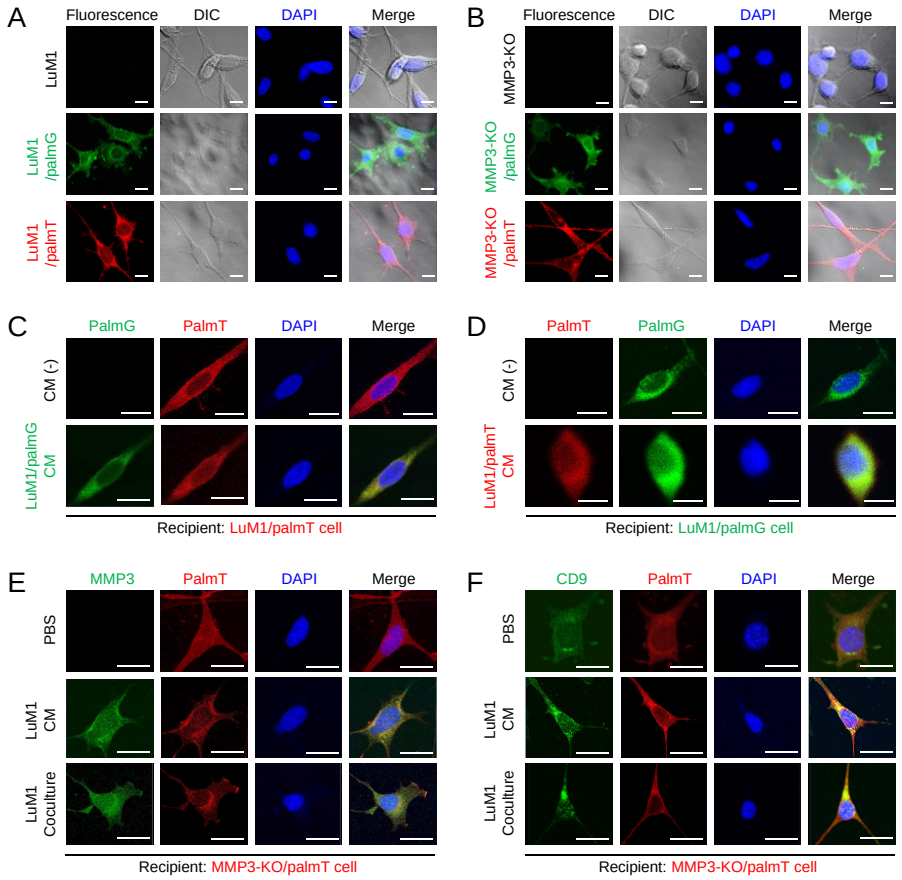

Figure 10. Establishment of fluorescent-labeled LuM1 and MMP3-KO cells. (A, B) Fluorescent labeled **(A)** LuM1 and **(B)** MMP3-KO cells. The stable cells were established by the transfection of expression constructs for palmT (red) and palmG (green) fluorescent proteins tagged with the palmitoylation signal. Images were taken using confocal laser scanning microscopy (CLSM). Non-fluorescent LuM1 and MMP3-KO cells were used as negative controls. **(C, D)** Molecular transfer of **(C)** palmG- and **(D)** palmT-labeled EVs from the conditioned medium (CM) of donor cells to recipient cells. **(C)** LuM1/palmT cells were treated with/without the CM of LuM1/palmG cells. **(D)** LuM1/palmG cells were treated with/without the CM of LuM1/palmT cells. **(E, F)** Immunostaining of **(E)** MMP3 and **(F)** CD9 in recipient MMP3-KO/palmT cells stimulated with PBS, LuM1-CM, or coculturing with LuM1 cells in

the Transwell system. DNA was stained with DAPI (blue). DIC, differential interference contrast. Scale bars, 20 μm. The experiments were repeated twice. (CM) collected under the 2D culture condition.

4.6. Penetration of MMP3-rich EVs into organoids

The bidirectional EVs-mediated transfer of cargo effectively influences the recipient phenotype to promote the development of an environment hospitable towards the cancer growth, invasion, and metastasis (Maacha et al. 2019). Moreover, the roles of EVs in the intercellular communication within the tumor microenvironment is increasingly acknowledged. Therefore, I examined whether MMP3 enriched EVs and CM was transferred and penetrating MMP3-null recipient tumoroids by immunohistochemistry. MMP3 was well detected on the surface and inside of the recipient tumoroids after the addition of LuM1-EVs and LuM1-CM (data not shown) (E.A. Taha et al., n.d.).

Additionally, MMP3-null tumoroids contained more space between cells and thus more fragile, while the addition of MMP3-rich, LuM1-EV, or –CM promoted the formation of solid tumoroids. To examine the molecular transfer and penetration of MMP3 into tumoroids, I next stained the recipient tumoroids by immunofluorescence (IF). To eliminate non-specific reaction, I confirmed the specificity of the anti-MMP3 antibody in the LuM1/palmT tumoroids (Figure S5).

To examine molecular penetration and tissue localization of MMP3, I used the CLSM. MMP3 from LuM1-EVs and –CM was found to penetrate the MMP3-null tumoroids (Figure 11A). Notably, intracellular and intranuclear penetration of MMP3 in the recipient

tumoroids was seen after the addition of MMP3-rich, LuM1-EVs (Figure 11A, B). MMP3 transferred from EVs and CM were seen as speckles in cytoplasm and nuclei in the recipient MMP3-null tumoroids (Figure 11B).

I have found that CD9 was decreased in MMP3-KO cells as shown in Figure 1 and Figure 7. Next, I examined whether CD9 could be altered in the CD9-low, MMP3-KO recipient tumoroids by adding LuM1-EVs or -CM. Indeed, CD9 was well stained in the recipient tumoroids, especially the parts close to the surface of tumoroids after the addition of the MMP3-rich CM or EVs (Figure 12A). Moreover, CD9 and endogenous palmT in the recipient tumoroids became abundantly expressed on the cell surface and well co-localized seen as honeycomb shape, suggesting that CD9 contributed to cell-cell adhesion in the recipient tumoroids (Figure 12B).

These findings indicate that LuM1-derived EVs and CM enhanced the solidity of MMP3-null tumoroids, which were relatively fragile. Additionally, MMP3 carried by LuM1-EVs was highly penetrative and deeply transferred to the recipient MMP3-null tumoroids. The intranuclear transfer of MMP3 and the increase in CD9 could contribute to the increased solidity in the MMP3-KO tumoroids.

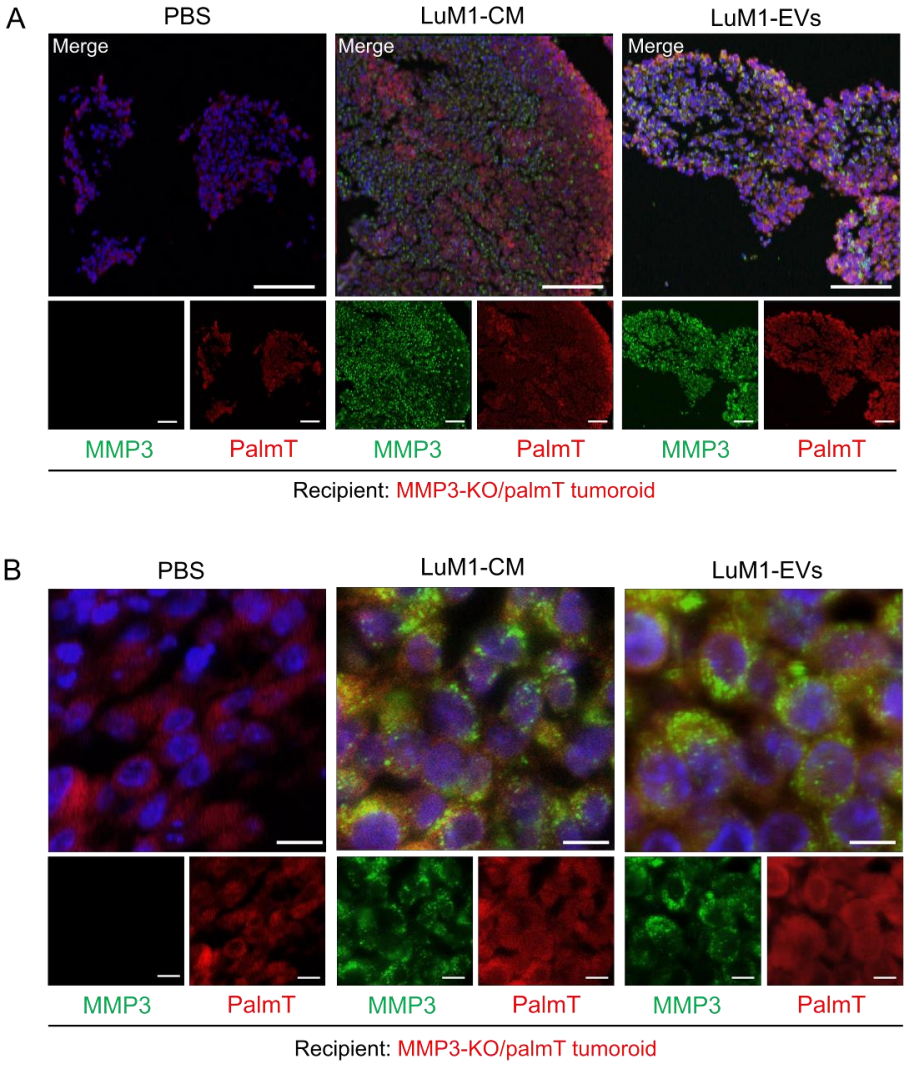

Figure 11. The EV-mediated deep transfer of MMP3 into tumoroids. MMP3-KO/palmT (red) tumoroids were treated with PBS, LuM1-CM, or LuM1-EVs for 24 h in the ULA-based 3D culture system. MMP3 (green) was stained by immunofluorescence. Nuclei were stained blue with DAPI. Images were taken by CLSM. **(A)** low and **(B)** high magnifications were shown. Scale bars; 100 μm (in low magnification images) and 10 μm (in high magnification images).

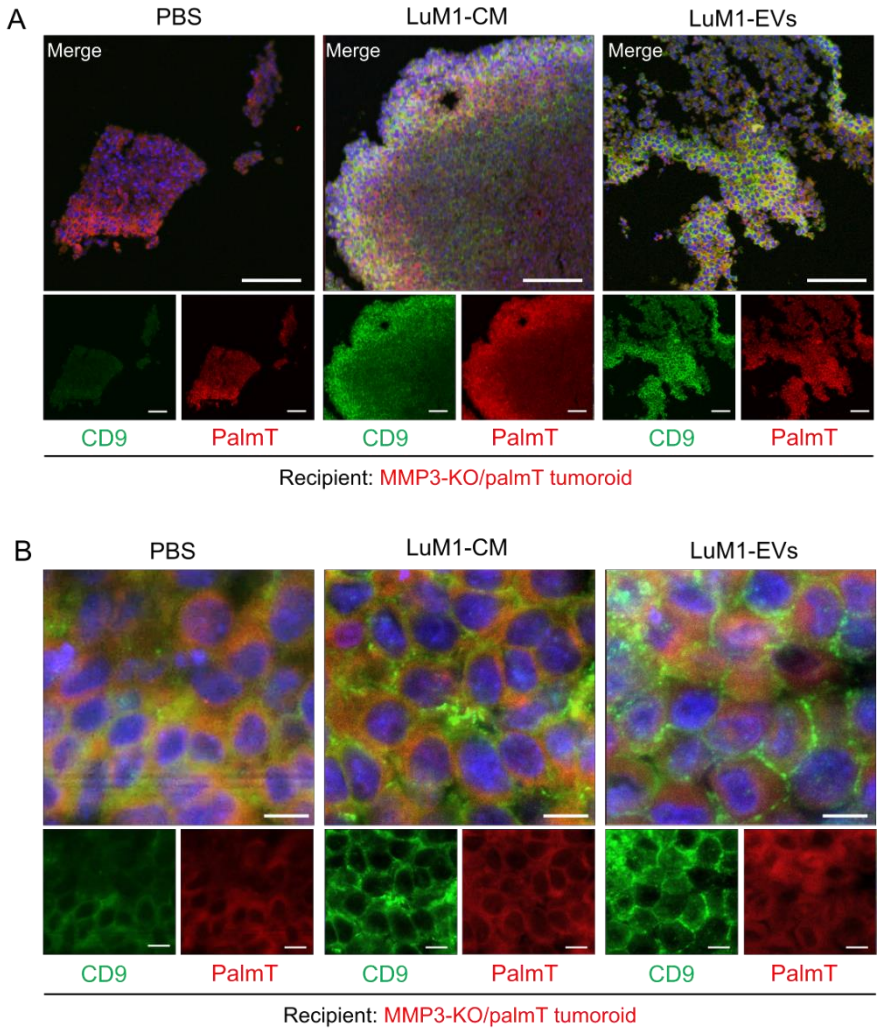

Figure 12. Treatment with LuM1-derived EVs and CM recovered CD9 in MMP3-null tumoroids. MMP3-KO/palmT (red) tumoroids were treated with PBS, LuM1-CM, or LuM1-EVs for 24 h in the ULA-based 3D culture system. CD9 (green) was stained by immunofluorescence. Nuclei were stained blue with DAPI. Images were taken by CLSM. **(A)** low and **(B)** high magnifications were shown. Scale bars; 100 μm (in low magnification images) and 10 μm (in high magnification images).

4.7. The knockout of the Mmp3 gene significantly decreased the transmissive potential of tumoroid-derived EVs

We have developed a method to examine the EV transfer to tumoroids by labeling EVs with red-fluorescent sphingolipids (Namba et al. 2018). In the present study, I monitored whether LuM1 tumoroid-derived or MMP3-KO tumoroid-derived heterogenous EVs (shown in Figure 4) were differently transferred to the MMP3-null tumoroids over 24 h.

I found that the MMP3-null tumoroids rapidly internalized the MMP3-rich, LuM1-EVs at a highly significant rate compared to the MMP3-null EV from 4 h to 24 h post-EVs addition (Figure 13A, B). Furthermore, the EVs uptake by tumoroids was increased in a time-dependent manner for 24 h (Figure 13B).

To sum up, these findings indicate that MMP3-rich, LuM1 tumoroid-derived EVs were highly transmissive and associated with tumoroids, while the loss of MMP3 in tumoroid-EVs reduced the transmissive and binding properties. These data also support our hypothesis that both endogenous and exogenous MMP3 play key roles in promoting the tumorigenesis, thereby MMP3-rich EVs were rapidly taken up by the MMP3-null tumoroids.

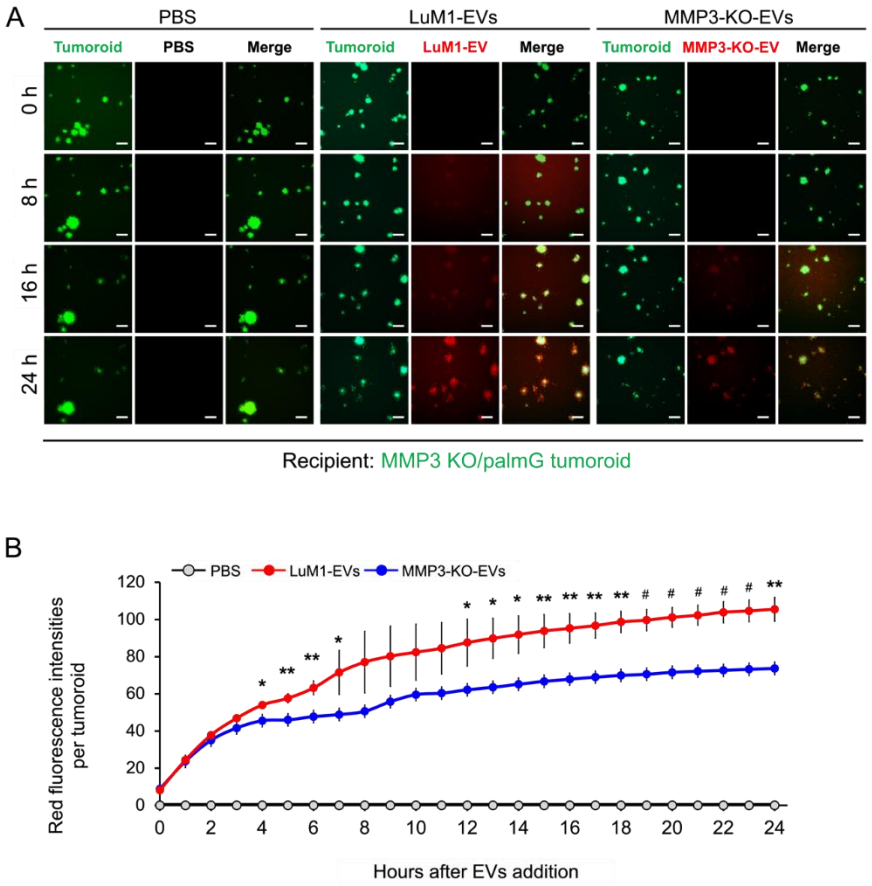

Figure 13. The Knockout of the MMP3 significantly decreased the transmissive potential of tumoroid-derived EVs. EVs were collected after 6 days from the culture supernatants of tumoroids that formed in ULA plates. EVs were fluorescently labeled with BODIPY TR Ceramide (red). The labeled EVs or PBS were added to the MMP3-KO/palmG (green) tumoroids at a concentration of 5 µg/mL in the NCP-based 3D culture with the stemness-enhancing medium. The uptake of EVs was monitored over 24 h using the high contents screening (HCS) system. **(A)** Time-course imaging of EV uptake (red) by MMP3-KO/palmG tumoroids (green) for 24 h. Scale bar, 100 µm. **(B)** Red fluorescence intensities of transmitted EVs in MMP3-KO/palmG tumoroids. The average fluorescence intensity of the PBS treatment group at time point 0 h was evaluated as

background and subtracted from raw values. n=3, *P<0.05, **P<0.01, and #P<0.001 (LuM1-EVs versus MMP3-KO-EVs).

4.8. MMP3-rich EVs and CM rescue the cell proliferation of MMP3-KO tumoroids

In the course of the present study, I compared the morphological characteristics of the LuM1 tumoroids versus MMP3-KO tumoroids by histological (H&E) staining. Five necrotic areas were observed in the MMP3-KO tumoroid, whereas only one small necrotic area was found in the LuM1 tumoroid (Figure 14A, B). The development of necrotic areas in the MMP3-KO tumoroid was at a higher percentage compared to the LuM1 tumoroid (15% versus 1% of the total area, respectively) (Figure 14A-C). The summed total and the percentage of necrotic areas were larger in the MMP3-KO tumoroids compared to their counterpart (Table 2).

Table 2. Necrotic areas in the LuM1 tumoroid versus MMP3-KO tumoroid

	LuM1	MMP3-KO
Total tumoroid area ($\mu m^{2)}$	331701	64148
Number of necrotic areas	1	5
Sum of necrotic areas	4807	9351
Necrosis %	1	15

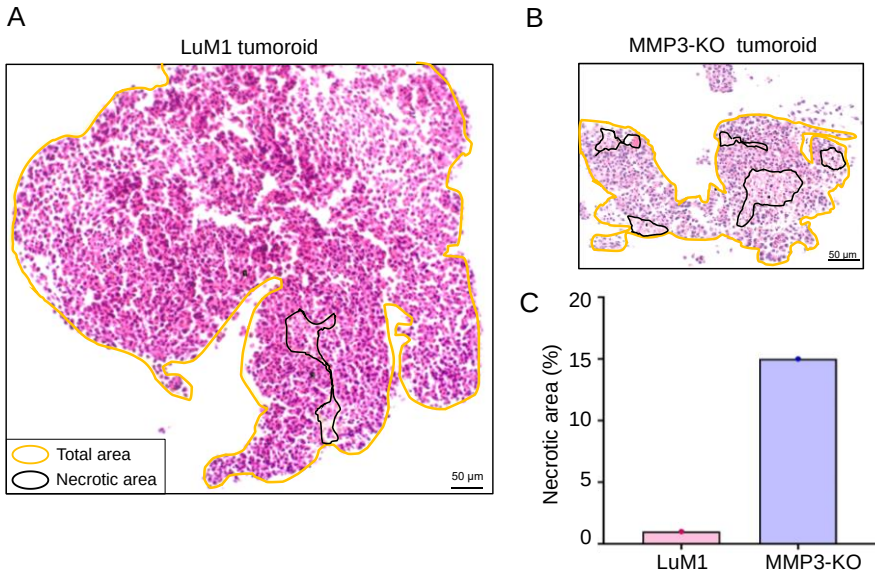

Figure 14. MMP3-knockout resulted in necrotic cell death in tumoroids. Tumoroids were cultured in the ULA-based 3D culture system with a stemness-enhancing medium for 8 days. **(A, B)** Hematoxylin and eosin (H&E) staining of **(A)** LuM1- and **(B)** MMP3-KO tumoroids. Necrotic areas were enclosed with black color, while the total tumoroids area was enclosed with yellow color. Scale bars, 50 µm. **(C)** The percentage of the necrotic areas in both tumoroids.

Additionally, there was a significant reduction in the Ki-67 expression, a marker of cell proliferation, in the MMP3-KO cells compared to their counterparts (Figure 15A, B). Following the addition of MMP3-rich CM and EVs, the recipient MMP3-KO tumoroid displayed a highly proliferative phenotype as judged by the highly significant increase in Ki-67 expression index (Figure 15A, B). These findings prove that MMP3 plays a crucial role in promoting cell proliferation in tumoroids and delaying the necrotic process.

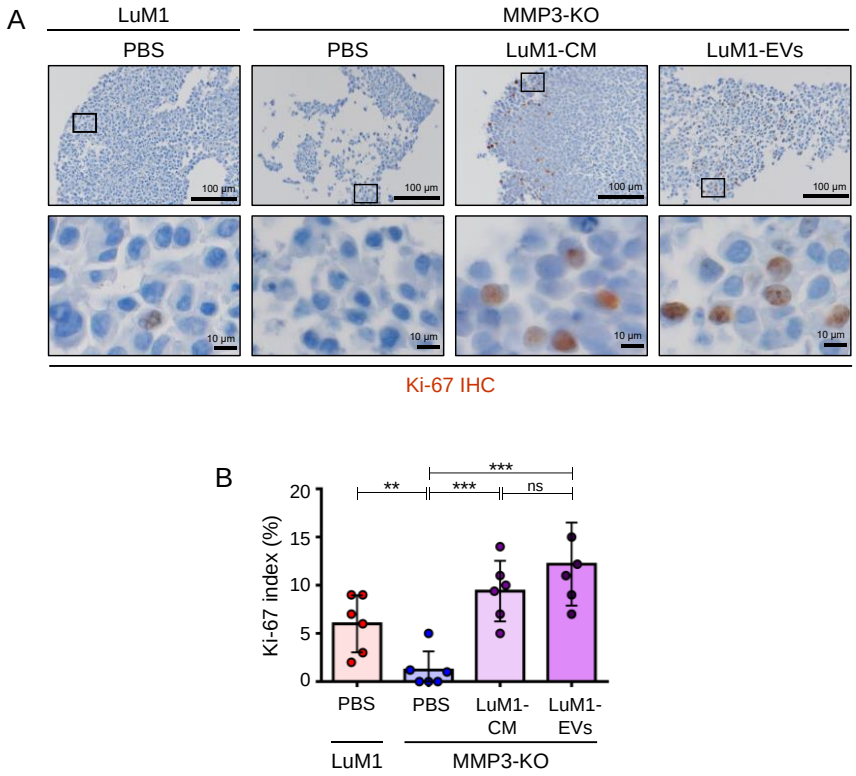

Figure 15. MMP3 enriched-EVs and CM rescue the proliferation of MMP3-KO tumoroids. LuM1-tumoroids or MMP3-KO tumoroids were treated with PBS, LuM1-CM, or LuM1-EVs for 24 h, and then Ki-67 was immunostained. (A) Ki-67 immunostaining (brown) in the LuM1 and MMP3-KO tumoroids. Scale bars, 100 μm (in low magnification images), and 10 μm (in high magnification images). (B) Ki-67 labeling index (%). n = 6, ** $p < 0.01$, *** $p < 0.001$; ns, not significant. Experiments were repeated twice.

5. Discussion

5.1. Summary

MMP3 is a proteolytic enzyme, as well as a transcriptional factor that plays a crucial role in tumor progression (Eguchi et al. 2008; Okusha et al. 2018; 2020) However, the roles of MMP3 within EVs had not unveiled before our study. We recently generated MMP3-KO cells by CRISPR/Cas9 system (Okusha et al. 2020) and have analyzed their properties in EVs and tumorigenesis.

In the current study, I found that MMP3 was abundantly detected in the high-metastatic cancer cells, their non-EV fluids, and EVs, although not in/from MMP3-KO cells. Thus, I newly explored (i) the oncogenic role of MMP3 on the *in vitro* tumoroid formation and on their EVs integrity under the 3D culture system, (ii) the tumorigenic potential of MMP3-rich versus MMP3-null EVs, and (iii) the EVs-mediated molecular transfer of MMP3 into the MMP3-KO tumoroids under the 3D culture system (Figure. 16).

5.2. Potential mechanism of how MMP3 promotes tumorigenesis

Our study indicates that MMP3 contained in EVs promotes primary tumorigenesis and metastasis also called secondary tumorigenesis. Several studies have reported that several MMP family members were packaged in EVs from body fluids or various types of cell lines (Dolo et al. 1999; Taraboletti et al. 2002; Belhocine et al. 2010; Shimoda and Khokha 2013; Reiner et al. 2017; Okusha et al. 2018). Our current results are consistent with recent data that LuM1-

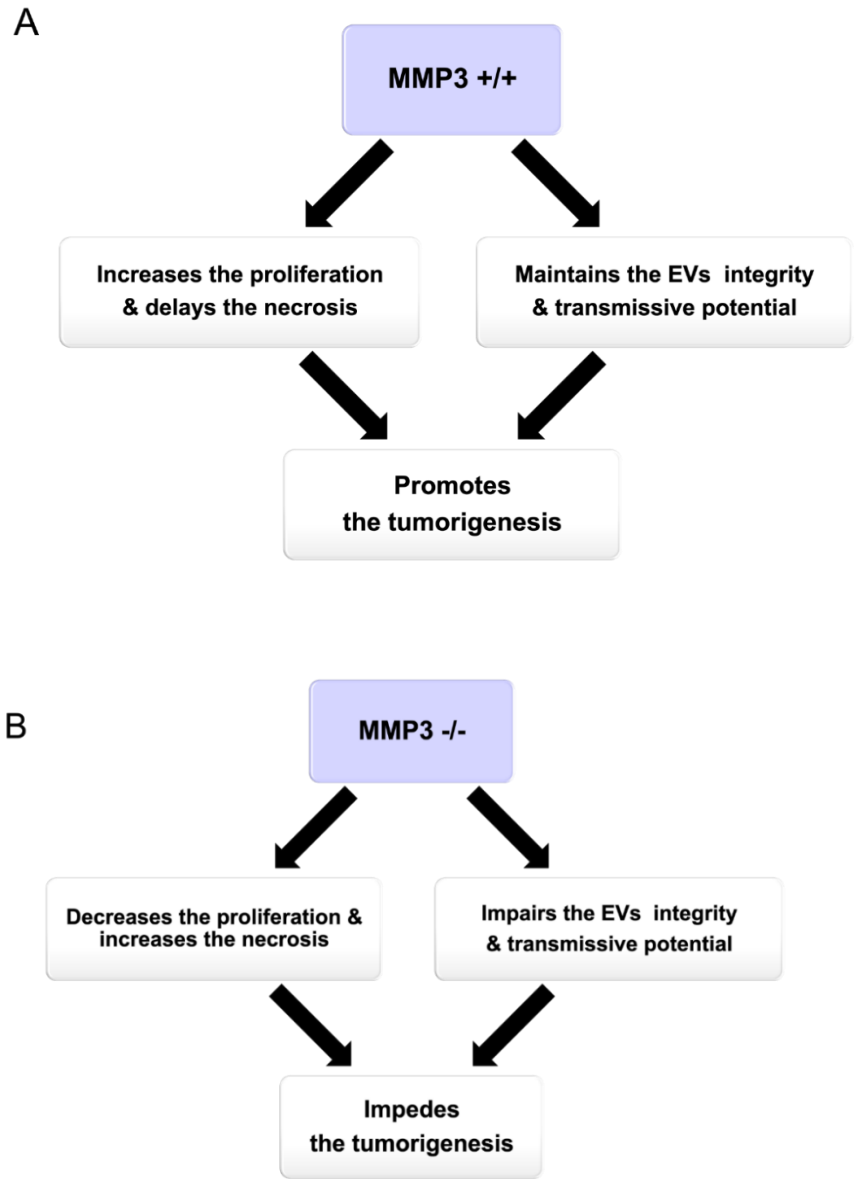

Figure. 16 Graphical abstracts summarizing the role of MMP3 on tumorigenesis *in vitro*. (A) Illustrating the net results in the presence of MMP3 (B) absence of MMP3 protein.

EVs (defined as oncosomes) enriched with MMP3 were highly transmissive and protumorigenic *in vitro* and *in vivo* (Okusha et al. 2020). MMP3 is one of the epithelial-to-mesenchymal transition (EMT) markers in cancer metastasis (Radisky and Radisky 2010), and it is well known that MMP3 makes cancer cells detached from solid mass and transferred to a distant region of the body (Okusha et al. 2018). In the current study, I focused on the roles of MMP3 in EVs of cancer cell lines for evaluating its tumorigenic potential.

As a potential mechanism of the tumorigenesis, MMP3 in EVs can penetrate to recipient cells resulting in inducing transformation (normal to cancer cells). We have shown that MMP3 could penetrate cell nuclei and transactivate connective tissue growth factor gene [CTGF aka cell communication network factor 2 (CCN2)] by interacting with DNA and heterochromatin proteins (HP1/CBXs) (Eguchi et al. 2008; Okusha et al. 2018). Moreover, we recently showed that MMP3 contained within EVs penetrate recipient cells and their nuclei (Okusha et al. 2020).

MMP3-rich EVs were able to transactivate the CCN2 gene promoter, while knockout of MMP3 from the EVs abolished this transactivating effect. The induction of CCN2 could be a key mechanism by which MMP3 induces transformation and tumor progression, as the stromal expression of CTGF promotes angiogenesis and prostate cancer tumorigenesis (F. Yang et al. 2005). Moreover, CCN2 modulates cell cycle progression through the upregulation of cyclin A (Kothapalli and Grotendorst 2000). Besides, CTGF is associated with oncogenic activities in glioblastoma by inducing the expression of the antiapoptotic proteins, Bcl-xl, surviving, and Flip (Yin et al. 2010). Thus, the protumorigenic effect

of MMP3 could be partially mediated by the induction of this multi-functional factor, CTGF.

Intranuclear MMP3 can also trans-activate HSP genes encoding cytoprotective factors, in collaboration with HP1/CBXs (Eguchi et al. 2017). Thus, intranuclearly translocated MMP3 could regulate broader intranuclear proteins and genes, some of which could be involved in cellular transformation such as EMT. Our current data indicated that MMP3 might also regulate CD9 and CD63 at transcriptional or post-transcriptional levels. The transactivating role of MMP3-EVs on the CCN2 gene was strictly mediated by a cis-element called TRENDIC (Okusha et al. 2020). Therefore, it would be important to verify which gene promoters contain TRENDIC-like motifs that are directly bound by MMP3. Some target genes regulated by MMP3 may involve cellular transformation.

Moreover, intranuclearly penetrating MMP3 could initiate cellular transformation by cleaving particular intranuclear proteins. It has become clear that the function of MMPs was not only restricted to degrade or inactivate matrix proteins and that proteolysis by MMPs can modulate or even increase functions of substrate proteins (Nelson et al. 2000).

Simultaneously, EV-associated MMP3 could activate extracellular transforming signals such as TGFβ by cleaving their pro-forms or inhibitory factors. Activities of many proteins are positively regulated by MMP proteolysis including CCN2/CTGF (Hashimoto et al. 2002; Kaasbøll et al. 2018; Okusha et al. 2020), insulin growth factor binding proteins (IGFBPs) heparin-binding epidermal growth factor (HB-EGF) (Suzuki et al. 1997), fibroblast growth factor receptor 1 (FGFR1) (Levi et al. 1996), interleukin-1beta (IL-1β) (Ito

et al. 1996), and tumor necrosis factor-alpha (TNF-α) (Haro et al. 2000). Such proteins activated by MMPs strengthen our *in vitro* findings that MMP3 can foster tumor development by modulating the activities of many signaling pathways and their receptors. Our research group is currently investigating such mechanisms of transformation induced by MMP3.

5.3. Potential role of MMP3 in cryoprotection

Our data suggest that MMP3 contained in EVs plays a cytoprotective role in tumors. Knockout of MMP3 markedly increased necrotic area in tumors thereby inhibited tumor growth. The addition of MMP3-rich EVs rescued tumor growth by increasing proliferating cells. Therefore, it is conceivable that MMP3 has cytoprotective and stimulates cell proliferation in tumors. Such cytoprotective and proliferative roles of MMP3 could be mediated by downstream factors such as HSPs and CTGF/CCN2 (Eguchi et al. 2008; 2017). We showed that intranuclear MMP3 can trans-activate HSP genes encoding cytoprotective factors, in collaboration with HP1/CBXs (Eguchi et al. 2017). Besides, CCN2 modulates cell cycle progression through the upregulation of cyclin A (Kothapalli and Grotendorst 2000).

Indeed, the MMP3-null tumoroid size was significantly smaller than their parental counterpart. Besides, the necrotic onset was occurring at a higher rate in the MMP3-null tumoroid compared to the LuM1 tumoroids. Necrosis is an accidental death of cells that are induced in response to extreme physiological conditions, such as hypoxia, toxin exposure, ischemia, reactive oxygen species exposure, nutrient deprivation, and extreme temperature changes (Walker et al.

1988; Nicotera, Leist, and Manzo 1999). Indeed, inside tumoroids/tumors are hypoxic and deprived of nutrients (Eguchi et al. 2018; Namba et al. 2018; Yoshida et al. 2019), although some cytoprotective factors could protect cells against necrotic cell death. Morphologically, necrotic cell death is characterized by swelling of the cellular organelles, a process of oncosis (also called ischemic cell death), and early plasma membrane rupture leading to loss of intracellular content (Parhamifar et al. 2014). The cell death observed in tumoroids in the current study fit the morphological criteria of necrosis.

Our data also indicated that MMP3 is a regulator for the physical and biological characteristics of EVs. Tetraspanins CD9 and CD63, category-1 EV markers, were downregulated in MMP3-null EVs compared to their counterparts (Figure 1E, F), suggesting that MMP3-knockout reduced the endogenous production or stability and subsequent release of CD9/CD63-contained EVs. It has been known that tetraspanins, CD326/EpCAM (these are category-1 EV markers), and the tight junction protein claudin-7 partners associate with each other for cell-cell adhesion and apoptosis resistance (Naour 2008). Moreover, tetraspanin interaction with another tetraspanin and integrins often depended on palmitoylation (Charrin et al. 2002; X. Yang et al. 2004). Therefore, MMP3-KO-triggered loss of CD9 and CD63 could reduce the cell-cell and EV-cell adhesions required for tumoroid integrity.

5.4. Release of L-EVs and s-EVs from 3D tumoroids

The morphological visualization of EVs showed abnormal disorganized shapes of EVs such as, crescent moon-like and broken EVs that were associated with the *Mmp3* loss. These data indicated that MMP3 is necessary for maintaining the stability of structural proteins required for the integrity of EVs.

Besides, we distinguished two subpopulations of 3D tumoroid-derived EVs, namely s-EVs (50-200 nm) and L-EVs (200-1000 nm). It is worth noting that, under the 2D culture system both LuM1 and MMP3-KO cells secreted homogeneous intact s-EVs (50-300 nm diameter) (Okusha et al. 2020). This inconsistency is due to our current study was performed under the 3D culture system which is completely different from the 2D culture system. Thus, intra-tumoral hypoxia developed under the 3D culture model may be stimulated the production of L-EVs. The release of both s-EVs and L-EVs might be a signature characteristic of the 3D tumoroids, a model resembling of tumors *in vivo.*

It has been reported that adipocytes secreted L-EVs containing cytoskeletal proteins and molecular chaperones, whereas s-EVs were shown to contain ECM proteins (Durcin et al. 2017). Moreover, the proteomic analysis of s- and L-EVs derived from a colorectal cancer cell line revealed that s-EVs were enriched with proteins associated with cell-matrix adhesion and cell-cell junctions (Jimenez et al. 2019). Similarly, s-EVs from fibrosarcoma cells showed similar enrichment for adhesion proteins (Jimenez et al. 2019). Likewise, one of our recent studies has demonstrated that the prostate cancer (PC-3) cells release two types of vesicles, s-EVs (30-200 nm) under a non-heated

condition, L-EVs (200-500 nm) and membrane-damaged EVs which were associated with HSP90α expression (Eguchi et al. 2020). Notably, both membrane-damaged EVs and L-EVs were co-released upon the heat shock stress, suggesting that vesicular membranes were damaged by the stress (Eguchi et al. 2020). Thus, the two different EVs populations may play distinct biological roles in the recipient cells. Our research group is currently challenging to separate the s- and L-EVs from the tumoroids and distinguish their properties.

5.5. Fluorescent labeling of EVs

To monitor the transmission and uptake of EVs between cells, I used two systems (i) PalmGFP and PalmtdTomato (Figure 10) or (ii) BODIPY TR ceramide labeled EVs (Figure 13). By utilizing the first system, I detected a robust fluorescent signal of donor-derived EVs in recipient cells, indicating that the bidirectional exchange of EVs between the cells.

Of note, PalmGFP and PalmtdTomato EV labeling strategy were designed to visualize and track multiple EV subtypes. Furthermore, by using these reporters, 0.22- and 0.8-μm sized EV populations, as well as sucrose density gradient with EV-marker proteins (such as Alix) were observed (Lai et al. 2015). Through the second EVs monitoring system, I tracked the uptake rate of MMP3-rich versus MMP3-null EVs for 24 h. An increase in BODIPY TR ceramide/EVs signal was noticed as early as 3 h post-EVs exposure period, and the increase continued until reached the saturation level after 24 h (Figure 13).

Thus, both fluorescent-EV monitoring systems were useful for monitoring the EV exchange. It has been shown that uptake of EVs

occurred via multiple routes, such as the direct fusion between EVs and the plasma membrane (Parolini et al. 2009), as well as EV internalization through lipid raft-, clathrin- and caveolae-dependent endocytosis, macropinocytosis, and phagocytosis (Morelli et al. 2004; Feng et al. 2010; Escrevente et al. 2011; Fitzner et al. 2011; Nanbo et al. 2013; Svensson et al. 2013). However, it is unclear which mechanism(s) is employed in different cell types under various conditions.

5.6. Inter MMPs regulation

Besides, EV-derived MMPs could promote proteolysis in recipient cells leading to tumor progression. Wang et al. indicated that EVs derived from adipocytes promoted lung cancer metastasis via transferring MMP3 that resulted in increasing the MMP9 activity in lung cancer cells (Wang et al. 2017). It has been shown that one MMP can activate another MMP including other members of MMPs. Therefore, the high expression of active MMP3 and/or MMP9 could activate other MMPs.

Indeed, I have shown that both MMP3 and MMP9 were expressed at high levels in LuM1 cells and proved their important role in tumor progression (Okusha et al. 2018). Nevertheless, the loss of MMP3 was crucial to reduce tumor and EV development. Our data indicate that exogenous MMP3 can be positioned at a higher level in the protease cascade that promotes tumor progression in the recipient cells.

6. Conclusion

Our study demonstrated that the loss-of-function of MMP3 significantly decreased the 3D-tumoroids formation *in vitro,* reduced tetraspanins (CD9 and CD63) in EVs and, resulted in destabilizing the EVs structural integrity. Moreover, I proved the successful labeling, exchanging of EVs between cells, and established a bidirectional EV transfer assay system. I confirmed the EVs-mediated molecular transfer of MMP3 into the MMP3-KO tumoroids under the 3D culture system. Also, I found that the addition of MMP3-enriched EVs (defined as oncosomes) fostered the tumorigenicity and increased the proliferation of MMP3-null cells. Thus MMP3-enriched oncosomes are highly transmissive and protumorigenic.

7. Supplementary Figures

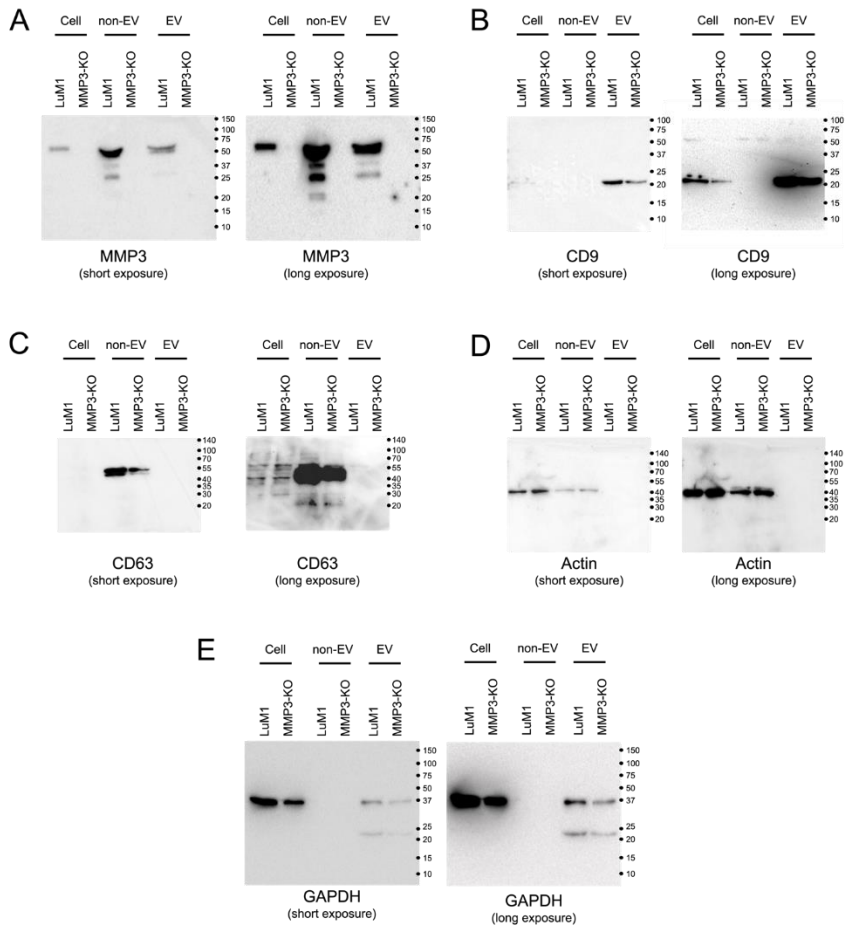

Figure S1. Full images of Western blotting of (A) MMP3, (B) CD9, (C) CD63, (D) β-actin, and (E) GAPDH, supporting Figure 1. Images from long and short exposure times are shown. The protein amount loaded from WCL and EV fractions was 10 µg per lane, while 5 µg per lane was loaded from the non-EV fractions.

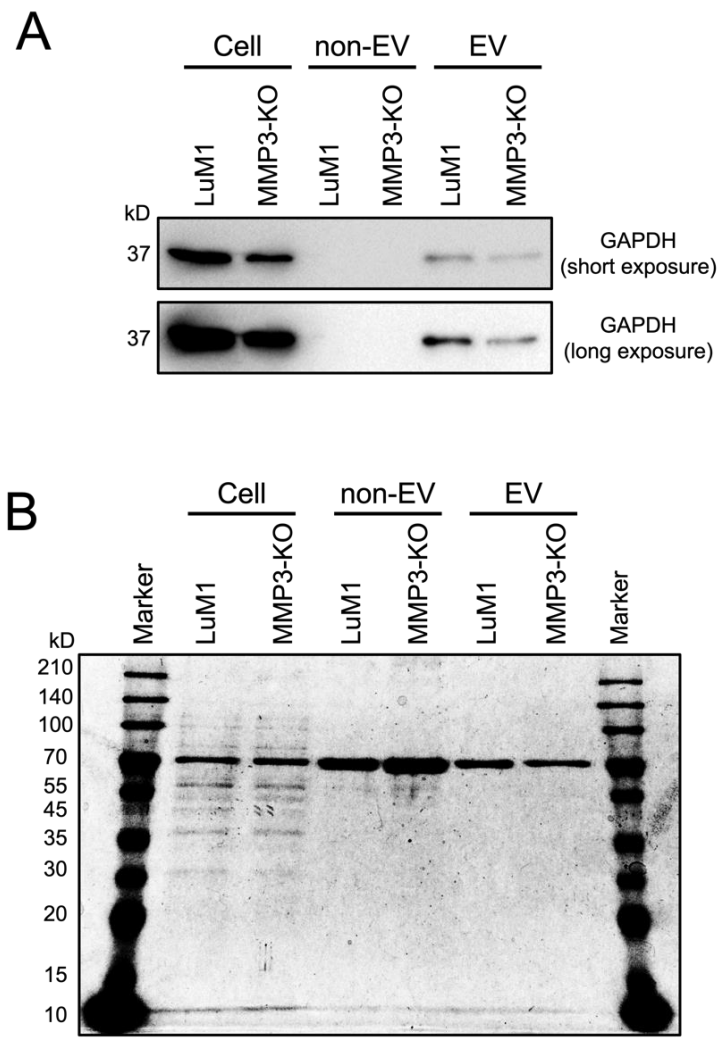

Figure S2. Images of (A) GAPDH Western blotting and (B) CBB staining of the SDS-PAGE. The amount of protein sample loaded for the CBB staining was 1μg per each lane.

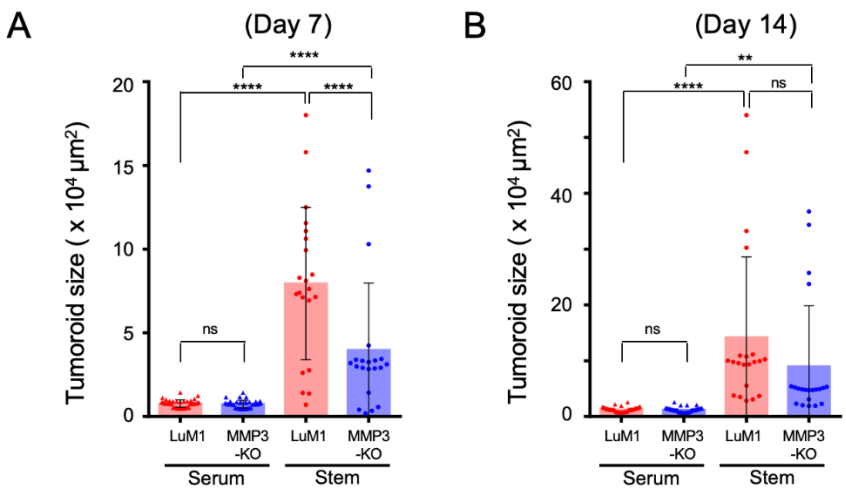

Figure S3. Column scatters plotting of the size of LuM1 tumoroids versus MMP3-KO tumoroids cultured for (A) 7 days or (B) 14 days in serum-containing or stemness media, supporting Figure 3. Data were represented as mean ± SD, n = 3, ** $p < 0.01$, **** $p < 0.0001$; ns, not significant.

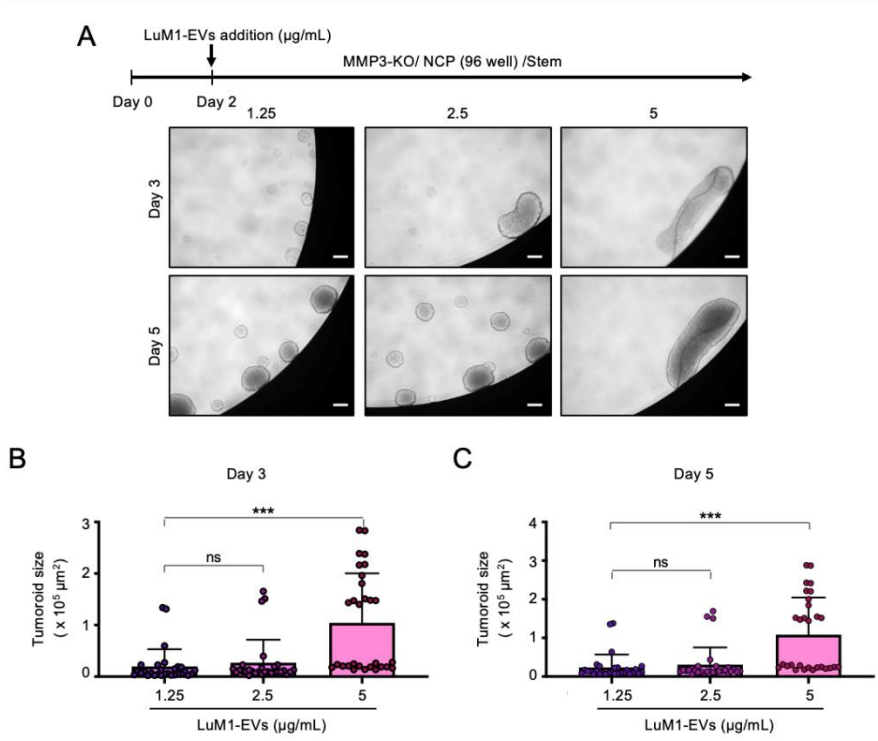

Figure S4. Evaluation of the effect of three different concentrations of LuM1-EVs on the MMP3-KO tumoroids growth. MMP3-KO tumoroids were treated with LuM1-EVs at a concentration of 1.25, 2.5, 5 µg/mL in the NCP-based 3D culture with the stemness-enhancing medium. Scale bar, 100 µm. (B, C) Tumoroid size quantification on (B) day 3 and (C) day 5 of the tumoroid formation periods. Data were represented as mean ± SD, n = 3, *** $p < 0.001$; ns, not significant.

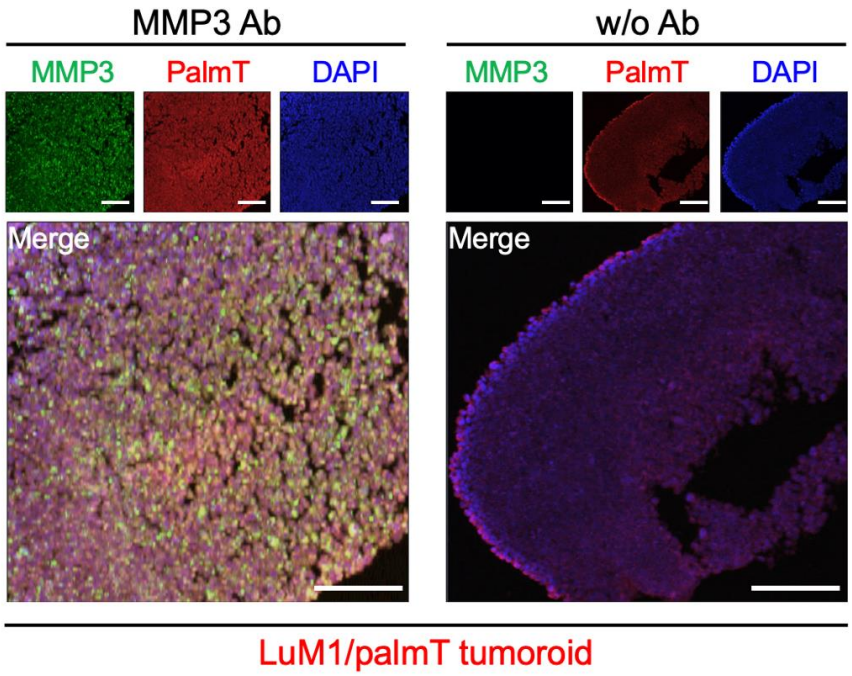

Figure S5. The specificity of the MMP3 antibody. (A, B) MMP3 expression (green) in (A) positive (B) and negative controls; LuM1/palmT tumoroids were stained with or without the MMP3 antibody, then stained with the secondary AF488 antibody. Nuclei were stained blue with DAPI. Images were taken by CLSM. w/o Ab; without antibody Scale bar 100 µm.

8. References

Abdouh, Mohamed, Matteo Floris, Zu-Hua Gao, Vincenzo Arena, Manuel Arena, and Goffredo Orazio Arena. 2019. "Colorectal Cancer-Derived Extracellular Vesicles Induce Transformation of Fibroblasts into Colon Carcinoma Cells." *Journal of Experimental & Clinical Cancer Research* 38 (1): 257. https://doi.org/10.1186/s13046-019-1248-2.

Akers, Johnny C., David Gonda, Ryan Kim, Bob S. Carter, and Clark C. Chen. 2013. "Biogenesis of Extracellular Vesicles (EV): Exosomes, Microvesicles, Retrovirus-like Vesicles, and Apoptotic Bodies." *Journal of Neuro-Oncology*.

https://doi.org/10.1007/s11060-013-1084-8.

Alkasalias, Twana, Lidia Moyano-Galceran, Marie Arsenian-Henriksson, and Kaisa Lehti. 2018. "Fibroblasts in the Tumor Microenvironment: Shield or Spear?" *International Journal of Molecular Sciences* 19 (5). https://doi.org/10.3390/ijms19051532.

Al-Nedawi, Khalid, Brian Meehan, Johann Micallef, Vladimir Lhotak, Linda May, Abhijit Guha, and Janusz Rak. 2008. "Intercellular Transfer of the Oncogenic Receptor EGFRvIII by Microvesicles Derived from Tumour Cells." *Nature Cell Biology* 10 (5): 619–24. https://doi.org/10.1038/ncb1725.

Andreola, Giovanna, Licia Rivoltini, Chiara Castelli, Veronica Huber, Paola Perego, Paola Deho, Paola Squarcina, et al. 2002. "Induction of Lymphocyte Apoptosis by Tumor Cell Secretion of FasL-Bearing Microvesicles." *Journal of Experimental Medicine* 195 (10): 1303–16. https://doi.org/10.1084/jem.20011624.

Arai, Kazuya, Takanori Eguchi, M. Mamunur Rahman, Ruriko Sakamoto, Norio Masuda, Tetsuya Nakatsura, Stuart K. Calderwood, Ken-ichi Kozaki, and Manabu Itoh. 2016. "A Novel High-Throughput 3D Screening System for EMT Inhibitors: A Pilot Screening Discovered the EMT Inhibitory Activity of CDK2 Inhibitor SU9516. *PLOS ONE* 11 (9): e0162394. https://doi.org/10.1371/journal.pone.0162394.

Babst, Markus. 2005. "A Protein's Final ESCRT." *Traffic* 6 (1): 2–9. https://doi.org/10.1111/j.1600-0854.2004.00246.x.

Babst, Markus. 2011. “MVB Vesicle Formation: ESCRT-Dependent, ESCRT-Independent and Everything in Between.” *Current Opinion in Cell Biology*. 23(4), 452–457. https://doi.org/10.1016/j.ceb.2011.04.008.

Balkwill, Frances R., Melania Capasso, and Thorsten Hagemann. 2012. “The Tumor Microenvironment at a Glance.” *Journal of Cell Science* 125 (23): 5591–96. https://doi.org/10.1242/jcs.116392.

Belhocine, M., T. Gernigon-Spychalowicz, M.-P. Jacob, Y. Benazzoug, and J.-M. Exbrayat. 2010. “Immunoexpression of Gelatinase (MMP-2 and MMP-9) in the Seminal Vesicles and Ventral Prostate of Libyan Jird (Meriones Libycus) during the Seasonal Cycle of Reproduction.” *Histology and Histopathology* 25 (5): 619–36. https://doi.org/10.14670/HH-25.619.

Berg, Gabriela, Magalí Barchuk, and Verónica Miksztowicz. 2019. “Behavior of Metalloproteinases in Adipose Tissue, Liver and Arterial Wall: An Update of Extracellular Matrix Remodeling.” *Cells* 8 (2): 158. https://doi.org/10.3390/cells8020158.

Bobrie, Angélique, Marina Colombo, Graça Raposo, and Clotilde Théry. 2011. “Exosome Secretion: Molecular Mechanisms and Roles in Immune Responses.” *Traffic*. Traffic. https://doi.org/10.1111/j.1600-0854.2011.01225.x.

Borges, F. T., L. A. Reis, and N. Schor. 2013. “Extracellular Vesicles: Structure, Function, and Potential Clinical Uses in Renal Diseases.” *Brazilian Journal of Medical and Biological Research* 2013 (46): 824–830. doi:10.1590/1414-431X20132964.

Borges, Fernanda T., Sonia A. Melo, Berna C. Özdemir, Noritoshi Kato, Ignacio Revuelta, Caroline A. Miller, Vincent H. Gattone, Valerie S. LeBleu, and Raghu Kalluri. 2013. “TGF-B1-Containing Exosomes from Injured Epithelial Cells Activate Fibroblasts to Initiate Tissue Regenerative Responses and Fibrosis.” *Journal of the American Society of Nephrology* 24 (3): 385–92. https://doi.org/10.1681/ASN.2012101031.

Boukouris, Stephanie, and Suresh Mathivanan. 2015. “Exosomes in Bodily Fluids Are a Highly Stable Resource of Disease

Biomarkers." *Proteomics. Clinical Applications* 9 (3–4): 358–67. https://doi.org/10.1002/prca.201400114.

Charrin, Stéphanie, Serge Manié, Michael Oualid, Martine Billard, Claude Boucheix, and Eric Rubinstein. 2002. "Differential Stability of Tetraspanin/Tetraspanin Interactions: Role of Palmitoylation." *FEBS Letters* 516 (1): 139–44. https://doi.org/10.1016/S0014-5793(02)02522-X.

Chen, Qiang, Jun-Jie Bei, Chuan Liu, Shi-Bin Feng, Wei-Bo Zhao, Zhou Zhou, Zheng-Ping Yu, Xiao-Jun Du, and Hou-Yuan Hu. 2016. "HMGB1 Induces Secretion of Matrix Vesicles by Macrophages to Enhance Ectopic Mineralization." *PLOS ONE* 11 (5): e0156686. https://doi.org/10.1371/journal.pone.0156686.

Choi, Dongsic, Cristiana Spinelli, Laura Montermini, and Janusz Rak. 2019. "Oncogenic Regulation of Extracellular Vesicle Proteome and Heterogeneity." *Proteomics* 19 (1-2). https://doi.org/10.1002/pmic.201800169.

Ciardiello, Chiara, Lorenzo Cavallini, Cristiana Spinelli, Julie Yang, Mariana Reis-Sobreiro, Paola de Candia, Valentina Minciacchi, and Dolores Di Vizio. 2016. "Focus on Extracellular Vesicles: New Frontiers of Cell-to-Cell Communication in Cancer." *International Journal of Molecular Sciences* 17 (2): 175. https://doi.org/10.3390/ijms17020175.

Coelho, Carolina, Lisa Brown, Maria Maryam, Raghav Vij, Daniel F.Q. Smith, Meagan C. Burnet, Jennifer E. Kyle, et al. 2019. "Listeria Monocytogenes Virulence Factors, Including Listeriolysin O, Are Secreted in Biologically Active Extracellular Vesicles." *Journal of Biological Chemistry* 294 (4): 1202–17. https://doi.org/10.1074/jbc.RA118.006472.

Colombo, Marina, Catarina Moita, Guillaume Van Niel, Joanna Kowal, James Vigneron, Philippe Benaroch, Nicolas Manel, Luis F. Moita, Clotilde Théry, and Graça Raposo. 2013. "Analysis of ESCRT Functions in Exosome Biogenesis, Composition and Secretion Highlights the Heterogeneity of Extracellular Vesicles." *Journal of Cell Science* 126 (24): 5553–65. https://doi.org/10.1242/jcs.128868.

Colombo, Marina, Graça Raposo, and Clotilde Théry. 2014. "Biogenesis, Secretion, and Intercellular Interactions of

Exosomes and Other Extracellular Vesicles." *Annual Review of Cell and Developmental Biology* 30: 255–89. https://doi.org/10.1146/annurev-cellbio-101512-122326.

Coussens, Lisa M., and Zena Werb. 1996. "Matrix Metalloproteinases and the Development of Cancer." *Chemistry and Biology* 3 (11): 895-904. https://doi.org/10.1016/S1074-5521(96)90178-7.

Curran, Stephanie, and Graeme I. Murray. 1999. "Matrix Metalloproteinases in Tumour Invasion and Metastasis." *The Journal of Pathology* 189 (3): 300–308. https://doi.org/10.1002/(SICI)1096-9896(199911)189:3<300::AID-PATH456>3.0.CO;2-C.

Di Vizio, Dolores, Matteo Morello, Andrew C. Dudley, Peter W. Schow, Rosalyn M. Adam, Samantha Morley, David Mulholland, et al. 2012. "Large Oncosomes in Human Prostate Cancer Tissues and in the Circulation of Mice with Metastatic Disease." *The American Journal of Pathology* 181 (5): 1573–84. https://doi.org/10.1016/j.ajpath.2012.07.030.

Dolo, Vincenza, Angela Ginestra, Donata Cassará, Giulio Ghersi, Hideaki Nagase, Maria Letizia Vittorelli, D Cassara, et al. 1999. "Shed Membrane Vesicles and Selective Localization of Gelatinases and MMP-9/TIMP-1 Complexes." *Annals of the New York Academy of Sciences* 878 (June): 497–99. https://doi.org/10.1111/j.1749-6632.1999.tb07707.x.

Durcin, Maëva, Audrey Fleury, Emiliane Taillebois, Grégory Hilairet, Zuzana Krupova, Céline Henry, Sandrine Truchet, et al. 2017. "Characterisation of Adipocyte-Derived Extracellular Vesicle Subtypes Identifies Distinct Protein and Lipid Signatures for Large and Small Extracellular Vesicles." *Journal of Extracellular Vesicles* 6 (1): 1305677. https://doi.org/10.1080/20013078.2017.1305677.

Duval, Kayla, Hannah Grover, Li-Hsin Han, Yongchao Mou, Adrian F. Pegoraro, Jeffery Fredberg, and Zi Chen. 2017. "Modeling Physiological Events in 2D vs. 3D Cell Culture." *Physiology (Bethesda, Md.)* 32 (4): 266–77. https://doi.org/10.1152/physiol.00036.2016.

Edmondson, Rasheena, Jessica Jenkins Broglie, Audrey F. Adcock, and Liju Yang. 2014. "Three-Dimensional Cell Culture Systems and Their Applications in Drug Discovery and Cell-

Based Biosensors." *Assay and Drug Development Technologies* 12 (4): 207–18. https://doi.org/10.1089/adt.2014.573.

Eguchi, T., Stuart K. Calderwood, Masaharu Takigawa, Satoshi Kubota, and Ken-ichi Kozaki. 2017. "Intracellular MMP3 Promotes *HSP* Gene Expression in Collaboration With Chromobox Proteins. *Journal of Cellular Biochemistry* 118 (1): 43–51. https://doi.org/10.1002/jcb.25607.

Eguchi, T., S. Kubota, K. Kawata, Y. Mukudai, J. Uehara, T. Ohgawara, S. Ibaragi, A. Sasaki, T. Kuboki, and M. Takigawa. 2008. "Novel Transcription Factor-Like Function of Human Matrix Metalloproteinase 3 Regulating the CTGF/CCN2 Gene." *Molecular and Cellular Biology* 28 (7): 2391–2413. https://doi.org/10.1128/MCB.01288-07.

Eguchi, T., Chiharu Sogawa, Yuka Okusha, Kenta Uchibe, Ryosuke Iinuma, Kisho Ono, Keisuke Nakano, et al. 2018. "Organoids with Cancer Stem Cell-like Properties Secrete Exosomes and HSP90 in a 3D Nanoenvironment." *PLOS ONE* 13 (2): e0191109. https://doi.org/10.1371/journal.pone.0191109.

Eguchi, T., Chiharu Sogawa, Kisho Ono, Masaki Matsumoto, Manh Tien Tran, Yuka Okusha, Benjamin J. Lang, Kuniaki Okamoto, and Stuart K. Calderwood. 2020. "Cell Stress Induced Stressome Release Including Damaged Membrane Vesicles and Extracellular HSP90 by Prostate Cancer Cells." *Cells* 9 (3): 755. https://doi.org/10.3390/cells9030755.

Elsayed, Maha, and Olivia M. Merkel. 2014. "Nanoimprinting of Topographical and 3D Cell Culture Scaffolds." *Nanomedicine* 9 (2): 349–66. https://doi.org/10.2217/nnm.13.200.

Escrevente, Cristina, Sascha Keller, Peter Altevogt, and Júlia Costa. 2011. "Interaction and Uptake of Exosomes by Ovarian Cancer Cells." *BMC Cancer* 11 (March): 108. https://doi.org/10.1186/1471-2407-11-108.

Fader, C. M., and M. I. Colombo. 2009. "Autophagy and Multivesicular Bodies: Two Closely Related Partners." *Cell Death and Differentiation*. Cell Death Differ. https://doi.org/10.1038/cdd.2008.168.

Feng, Du, Wen-Long Zhao, Yun-Ying Ye, Xiao-Chen Bai, Rui-Qin Liu, Lei-Fu Chang, Qiang Zhou, and Sen-Fang Sui. 2010. "Cellular Internalization of Exosomes Occurs Through

Phagocytosis." *Traffic* 11 (5): 675–87. https://doi.org/10.1111/j.1600-0854.2010.01041.x.

Fitzner, Dirk, Mareike Schnaars, Denise van Rossum, Gurumoorthy Krishnamoorthy, Payam Dibaj, Mostafa Bakhti, Tommy Regen, Uwe-Karsten Hanisch, and Mikael Simons. 2011. "Selective Transfer of Exosomes from Oligodendrocytes to Microglia by Macropinocytosis." *Journal of Cell Science* 124 (3): 447–58. https://doi.org/10.1242/jcs.074088.

Fujiwara, Toshifumi, Takanori Eguchi, Chiharu Sogawa, Kisho Ono, Jun Murakami, Soichiro Ibaragi, Jun-ichi Asaumi, Stuart K. Calderwood, Kuniaki Okamoto, and Ken-ichi Kozaki. 2018. "Carcinogenic Epithelial-Mesenchymal Transition Initiated by Oral Cancer Exosomes Is Inhibited by Anti-EGFR Antibody Cetuximab." *Oral Oncology* 86 (November): 251–57. https://doi.org/10.1016/j.oraloncology.2018.09.030.

Galea, Charles A, Hai M Nguyen, K George Chandy, Brian J Smith, and Raymond S Norton. 2014. "Domain Structure and Function of Matrix Metalloprotease 23 (MMP23): Role in Potassium Channel Trafficking." *Cellular and Molecular Life Sciences : CMLS* 71 (7): 1191–1210. https://doi.org/10.1007/s00018-013-1431-0.

Gialeli, Chrisostomi, Achilleas D. Theocharis, and Nikos K. Karamanos. 2011. "Roles of Matrix Metalloproteinases in Cancer Progression and Their Pharmacological Targeting." *The FEBS Journal* 278 (1): 16–27. https://doi.org/10.1111/j.1742-4658.2010.07919.x.

Giusti, Ilaria, Marianna Di Francesco, Sandra D'Ascenzo, Maria Grazia Palmerini, Guido Macchiarelli, Gaspare Carta, and Vincenza Dolo. 2018. "Ovarian Cancer-Derived Extracellular Vesicles Affect Normal Human Fibroblast Behavior." *Cancer Biology & Therapy* 19 (8): 722–34. https://doi.org/10.1080/15384047.2018.1451286.

Golubkov, Vladislav S., Alexei V. Chekanov, P. Cieplak, Alexander E. Aleshin, Andrei V. Chernov, Wenhong Zhu, Ilian A. Radichev, Danhua Zhang, P. Duc Dong, and Alex Y. Strongin. 2010. "The Wnt/Planar Cell Polarity Protein-Tyrosine Kinase-7 (PTK7) Is a Highly Efficient Proteolytic Target of Membrane Type-1 Matrix Metalloproteinase: Implications in Cancer and Embryogenesis." *Journal of Biological Chemistry*

285 (46): 35740–49. https://doi.org/10.1074/jbc.M110.165159.

Griffith, Linda G., and Melody A. Swartz. 2006. "Capturing Complex 3D Tissue Physiology in Vitro." *Nature Reviews. Molecular Cell Biology* 7 (3): 211–24. https://doi.org/10.1038/nrm1858.

Ha, Dinh, Ningning Yang, and Venkatareddy Nadithe. 2016. "Exosomes as Therapeutic Drug Carriers and Delivery Vehicles across Biological Membranes: Current Perspectives and Future Challenges." *Acta Pharmaceutica Sinica B* 6 (4): 287–96. https://doi.org/10.1016/j.apsb.2016.02.001.

Haro, H., H. C. Crawford, B. Fingleton, K. Shinomiya, D. M. Spengler, and L. M. Matrisian. 2000. "Matrix Metalloproteinase-7-Dependent Release of Tumor Necrosis Factor-Alpha in a Model of Herniated Disc Resorption." *The Journal of Clinical Investigation* 105 (2): 143–50. https://doi.org/10.1172/JCI7091.

Hashimoto, Gakuji, Isao Inoki, Yutaka Fujii, Takanori Aoki, Eiji Ikeda, and Yasunori Okada. 2002. "Matrix Metalloproteinases Cleave Connective Tissue Growth Factor and Reactivate Angiogenic Activity of Vascular Endothelial Growth Factor 165." *Journal of Biological Chemistry* 277 (39): 36288–95. https://doi.org/10.1074/jbc.M201674200.

Hendrix, An, Dawn Maynard, Patrick Pauwels, Geert Braems, Hannelore Denys, Rudy Van den Broecke, Jo Lambert, et al. 2010. "Effect of the Secretory Small GTPase Rab27B on Breast Cancer Growth, Invasion, and Metastasis." *Journal of the National Cancer Institute* 102 (12): 866–80. https://doi.org/10.1093/jnci/djq153.

Higginbotham, James N., Michelle Demory Beckler, Jonathan D. Gephart, Jeffrey L. Franklin, Galina Bogatcheva, Gert-Jan Kremers, David W. Piston, et al. 2011. "Amphiregulin Exosomes Increase Cancer Cell Invasion." *Current Biology: CB* 21 (9): 779–86. https://doi.org/10.1016/j.cub.2011.03.043.

Hiratsuka, Sachie, Kazuhiro Nakamura, Shinobu Iwai, Masato Murakami, Takeshi Itoh, Hiroshi Kijima, J. Michael Shipley, Robert M Senior, and Masabumi Shibuya. 2002. "MMP9 Induction by Vascular Endothelial Growth Factor Receptor-1

Is Involved in Lung-Specific Metastasis." *Cancer Cell* 2 (4): 289–300. https://doi.org/10.1016/S1535-6108(02)00153-8.

Hirschhaeuser, Franziska, Heike Menne, Claudia Dittfeld, Jonathan West, Wolfgang Mueller-Klieser, and Leoni A. Kunz-Schughart. 2010. "Multicellular Tumor Spheroids: An Underestimated Tool Is Catching up Again." *Journal of Biotechnology* 148 (1): 3–15. https://doi.org/10.1016/j.jbiotec.2010.01.012.

Huang, Yuwei, Ben Zucker, Shaojin Zhang, Sharon Elias, Yun Zhu, Hui Chen, Tianlun Ding, et al. 2019. "Migrasome Formation Is Mediated by Assembly of Micron-Scale Tetraspanin Macrodomains." *Nature Cell Biology* 21 (8): 991–1002. https://doi.org/10.1038/s41556-019-0367-5.

Ito, A., A. Mukaiyama, Y. Itoh, H. Nagase, I. B. Thogersen, J. J. Enghild, Y. Sasaguri, and Y. Mori. 1996. "Degradation of Interleukin 1beta by Matrix Metalloproteinases." *The Journal of Biological Chemistry* 271 (25): 14657–60. https://doi.org/10.1074/jbc.271.25.14657.

Jakhar, Rekha, and Karen Crasta. 2019. "Exosomes as Emerging Pro-Tumorigenic Mediators of the Senescence-Associated Secretory Phenotype." *International Journal of Molecular Sciences* 20 (10), 2547. https://doi.org/10.3390/ijms20102547.

Janowska-Wieczorek, Anna, Marcin Wysoczynski, Jacek Kijowski, Leah Marquez-Curtis, Bogdan Machalinski, Janina Ratajczak, and Mariusz Z. Ratajczak. 2005. "Microvesicles Derived from Activated Platelets Induce Metastasis and Angiogenesis in Lung Cancer." *International Journal of Cancer* 113 (5): 752–60. https://doi.org/10.1002/ijc.20657.

Jimenez, Lizandra, Hui Yu, Andrew J. McKenzie, Jeffrey L. Franklin, James G. Patton, Qi Liu, and Alissa M. Weaver. 2019. "Quantitative Proteomic Analysis of Small and Large Extracellular Vesicles (EVs) Reveals Enrichment of Adhesion Proteins in Small EVs." *Journal of Proteome Research* 18 (3): 947–59. https://doi.org/10.1021/acs.jproteome.8b00647.

Kaasbøll, Ole Jørgen, Ashish K. Gadicherla, Jian-Hua Wang, Vivi Talstad Monsen, Else Marie Valbjørn Hagelin, Meng-Qiu Dong, and Håvard Attramadal. 2018. "Connective Tissue Growth Factor (CCN2) Is a Matricellular Preproprotein

Controlled by Proteolytic Activation." *The Journal of Biological Chemistry* 293 (46): 17953–70. https://doi.org/10.1074/jbc.RA118.004559.

Kessenbrock, Kai, Vicki Plaks, and Zena Werb. 2010. "Matrix Metalloproteinases: Regulators of the Tumor Microenvironment." *Cell* 141 (1): 52–67. https://doi.org/10.1016/j.cell.2010.03.015.

Kim, Oh Youn, Hyun Taek Park, Nhung Thi Hong Dinh, Seng Jin Choi, Jaewook Lee, Ji Hyun Kim, Seung Woo Lee, and Yong Song Gho. 2017. "Bacterial Outer Membrane Vesicles Suppress Tumor by Interferon-γ-Mediated Antitumor Response." *Nature Communications* 8 (1): 626. https://doi.org/10.1038/s41467-017-00729-8.

Koshikawa, Naohiko, Tomoko Minegishi, Andrew Sharabi, Vito Quaranta, and Motoharu Seiki. 2005. "Membrane-Type Matrix Metalloproteinase-1 (MT1-MMP) Is a Processing Enzyme for Human Laminin Γ2 Chain." *Journal of Biological Chemistry* 280 (1): 88–93. https://doi.org/10.1074/jbc.M411824200.

Koshikawa, Naohiko, Hiroto Mizushima, Tomoko Minegishi, Ryo Iwamoto, Eisuke Mekada, and Motoharu Seiki. 2010. "Membrane Type 1-Matrix Metalloproteinase Cleaves off the NH 2-Terminal Portion of Heparin-Binding Epidermal Growth Factor and Converts It into a Heparin-Independent Growth Factor." *Cancer Research* 70 (14): 6093–6103. https://doi.org/10.1158/0008-5472.CAN-10-0346.

Kothapalli, D., and G. R. Grotendorst. 2000. "CTGF Modulates Cell Cycle Progression in CAMP-Arrested NRK Fibroblasts." *Journal of Cellular Physiology* 182 (1): 119–26. https://doi.org/10.1002/(SICI)1097-4652(200001)182:1<119::AID-JCP13>3.0.CO;2-4.

Lai, Charles P, Edward Y Kim, Christian E Badr, Ralph Weissleder, Thorsten R Mempel, Bakhos A Tannous, and Xandra O Breakefield. 2015. "Multiplexed Reporters." *Nature Communications* 6 (May): 1–12. https://doi.org/10.1038/ncomms8029.

Lawson, Charlotte, Jose M. Vicencio, Derek M. Yellon, and Sean M. Davidson. 2016. "Microvesicles and Exosomes: New Players in Metabolic and Cardiovascular Disease." *Journal of*

Endocrinology 228 (2): R57–71. https://doi.org/10.1530/JOE-15-0201.

Levi, E, R Fridman, H Q Miao, Y S Ma, A Yayon, and I Vlodavsky. 1996. "Matrix Metalloproteinase 2 Releases Active Soluble Ectodomain of Fibroblast Growth Factor Receptor 1." *Proceedings of the National Academy of Sciences of the United States of America* 93 (14): 7069–74.

Lu, Pengfei, Ken Takai, Valerie M. Weaver, and Zena Werb. 2011. "Extracellular Matrix Degradation and Remodeling in Development and Disease." *Cold Spring Harbor Perspectives in Biology* 3 (12). https://doi.org/10.1101/cshperspect.a005058.

Lubbe, Wilhelm J., Zengyi Y. Zhou, Weili Fu, David Zuzga, Stephanie Schulz, Rafael Fridman, Ruth J. Muschel, Scott A. Waldman, and Giovanni M. Pitari. 2006. "Tumor Epithelial Cell Matrix Metalloproteinase 9 Is a Target for Antimetastatic Therapy in Colorectal Cancer." *Clinical Cancer Research* 12 (6): 1876–82. https://doi.org/10.1158/1078-0432.CCR-05-2686.

Lv, Donglai, Zongtao Hu, Lin Lu, Husheng Lu, and Xiuli Xu. 2017. "Three-Dimensional Cell Culture: A Powerful Tool in Tumor Research and Drug Discovery." *Oncology Letters* 14 (6): 6999–7010. https://doi.org/10.3892/ol.2017.7134.

Ma, Liang, Ying Li, Junya Peng, Danni Wu, Xiaoxin Zhao, Yitong Cui, Lilian Chen, Xiaojun Yan, Yanan Du, and Li Yu. 2015. "Discovery of the Migrasome, an Organelle Mediating Release of Cytoplasmic Contents during Cell Migration." *Cell Research* 25 (1): 24–38. https://doi.org/10.1038/cr.2014.135.

Maacha, Selma, Ajaz A. Bhat, Lizandra Jimenez, Afsheen Raza, Mohammad Haris, Shahab Uddin, and Jean-Charles Grivel. 2019. "Extracellular Vesicles-Mediated Intercellular Communication: Roles in the Tumor Microenvironment and Anti-Cancer Drug Resistance." *Molecular Cancer* 18 (1): 55. https://doi.org/10.1186/s12943-019-0965-7.

Mañes, Santos, Mercedes Llorente, Rosa Ana Lacalle, Concepción Gómez-Moutón, Leonor Kremer, Emilia Mira, and Carlos Martínez-A. 1999. "The Matrix Metalloproteinase-9 Regulates the Insulin-like Growth Factor- Triggered Autocrine Response in DU-145 Carcinoma Cells." *Journal of*

Biological Chemistry 274 (11): 6935–45. https://doi.org/10.1074/jbc.274.11.6935.

Mañes, Santos, Emilia Mira, Maria Del Mar Barbacid, Angel Ciprés, Piedad Fernández-Resa, Jose María Buesa, Isabel Mérida, Miguel Aracil, Gabriel Márquez, and Carlos Martínez-A. 1997. "Identification of Insulin-like Growth Factor-Binding Protein-1 as a Potential Physiological Substrate for Human Stromelysin-3." *Journal of Biological Chemistry* 272 (41): 25706–12. https://doi.org/10.1074/jbc.272.41.25706.

Mathivanan, Suresh, Hong Ji, and Richard J. Simpson. 2010. "Exosomes: Extracellular Organelles Important in Intercellular Communication." *Journal of Proteomics* 73 (10): 1907-20. https://doi.org/10.1016/j.jprot.2010.06.006.

Mebarek, Saida, Abdelkarim Abousalham, David Magne, Le Duy Do, Joanna Bandorowicz-Pikula, Slawomir Pikula, and René Buchet. 2013. "Phospholipases of Mineralization Competent Cells and Matrix Vesicles: Roles in Physiological and Pathological Mineralizations." *International Journal of Molecular Sciences 14 (3) 5036-129.* https://doi.org/10.3390/ijms14035036.

Mikhailova, Margarita, Xiaoping Xu, Trista K Robichaud, Sanjay Pal, Gregg B Fields, and Bjorn Steffensen. 2012. "Identification of Collagen Binding Domain Residues That Govern Catalytic Activities of Matrix Metalloproteinase-2 (MMP-2)." *Matrix Biology : Journal of the International Society for Matrix Biology* 31 (7–8): 380–88. https://doi.org/10.1016/j.matbio.2012.10.001.

Morelli, Adrian E., Adriana T. Larregina, William J. Shufesky, Mara L. G. Sullivan, Donna Beer Stolz, Glenn D. Papworth, Alan F. Zahorchak, et al. 2004. "Endocytosis, Intracellular Sorting, and Processing of Exosomes by Dendritic Cells." *Blood* 104 (10): 3257–66. https://doi.org/10.1182/blood-2004-03-0824.

Murphy, G, Q Nguyen, M I Cockett, S J Atkinson, J A Allan, C G Knight, F Willenbrock, and A J Docherty. 1994. "Assessment of the Role of the Fibronectin-like Domain of Gelatinase A by Analysis of a Deletion Mutant." *The Journal of Biological Chemistry* 269 (9): 6632–36.

Nagaset, Hideaki, and J. Frederick Woessner. 1999. "Matrix Metalloproteinases." *Journal of Biological Chemistry* 274 (31): 21491-4. https://doi.org/10.1074/jbc.274.31.21491.

Namba, Yuri, Chiharu Sogawa, Yuka Okusha, Hotaka Kawai, Mami Itagaki, Kisho Ono, Jun Murakami, et al. 2018. "Depletion of Lipid Efflux Pump ABCG1 Triggers the Intracellular Accumulation of Extracellular Vesicles and Reduces Aggregation and Tumorigenesis of Metastatic Cancer Cells." *Frontiers in Oncology* 8 (OCT): 1–16. https://doi.org/10.3389/fonc.2018.00376.

Nanbo, Asuka, Eri Kawanishi, Ryuji Yoshida, and Hironori Yoshiyama. 2013. "Exosomes Derived from Epstein-Barr Virus-Infected Cells Are Internalized via Caveola-Dependent Endocytosis and Promote Phenotypic Modulation in Target Cells." *Journal of Virology* 87 (18): 10334–47. https://doi.org/10.1128/JVI.01310-13.

Naour, Francois Le. 2008. "The Tumor Antigen Epcam: Tetraspanins and the Tight Junction Protein Claudin-7, New Partners, New Functions." *Frontiers in Bioscience* 13: 5847–5865. https://doi.org/10.2741/3121.

Nelson, A. R., B. Fingleton, M. L. Rothenberg, and L. M. Matrisian. 2000. "Matrix Metalloproteinases: Biologic Activity and Clinical Implications." *Journal of Clinical Oncology* 18 (5): 1135–49. https://doi.org/10.1200/JCO.2000.18.5.1135.

Nicotera, P., M. Leist, and L. Manzo. 1999. "Neuronal Cell Death: A Demise with Different Shapes." *Trends in Pharmacological Sciences* 20 (2): 46–51. https://doi.org/10.1016/s0165-6147(99)01304-8.

Niel, Guillaume Van, Gisela D'Angelo, and Graça Raposo. 2018. "Shedding Light on the Cell Biology of Extracellular Vesicles." *Nature Reviews Molecular Cell Biology* 19 (4) 213-28. https://doi.org/10.1038/nrm.2017.125.

Okusha, Yuka, Takanori Eguchi, Chiharu Sogawa, Tatsuo Okui, Keisuke Nakano, Kuniaki Okamoto, and Ken-Ichi Kozaki. 2018. "The Intranuclear PEX Domain of MMP Involves Proliferation, Migration, and Metastasis of Aggressive Adenocarcinoma Cells." *Journal of Cellular Biochemistry* 119 (9): 7363–76. https://doi.org/10.1002/jcb.27040.

Okusha, Yuka, Takanori Eguchi, Manh T. Tran, Chiharu Sogawa, Kaya Yoshida, Mami Itagaki, Eman A. Taha, et al. 2020. "Extracellular Vesicles Enriched with Moonlighting Metalloproteinase Are Highly Transmissive, Pro-Tumorigenic, and Trans-Activates Cellular Communication Network Factor (CCN2/CTGF): CRISPR against Cancer." *Cancers* 12 (4): 881. https://doi.org/10.3390/cancers12040881.

Ono, Kisho, Takanori Eguchi, Chiharu Sogawa, Stuart K. Calderwood, Junya Futagawa, Tomonari Kasai, Masaharu Seno, Kuniaki Okamoto, Akira Sasaki, and Ken-ichi Kozaki. 2018. "HSP-Enriched Properties of Extracellular Vesicles Involve Survival of Metastatic Oral Cancer Cells." *Journal of Cellular Biochemistry* 119 (9): 7350–62. https://doi.org/10.1002/jcb.27039.

Parhamifar, Ladan, Helene Andersen, Linping Wu, Arnaldur Hall, Diana Hudzech, and Seyed Moien Moghimi. 2014. "Chapter Twelve - Polycation-Mediated Integrated Cell Death Processes." In *Advances in Genetics* 88:353–98. https://doi.org/10.1016/B978-0-12-800148-6.00012-2.

Parolini, Isabella, Cristina Federici, Carla Raggi, Luana Lugini, Simonetta Palleschi, Angelo De Milito, Carolina Coscia, et al. 2009. "Microenvironmental PH Is a Key Factor for Exosome Traffic in Tumor Cells." *Journal of Biological Chemistry* 284 (49): 34211–22. https://doi.org/10.1074/jbc.M109.041152.

Peng, Wen Jia, Jun Wei Yan, Ya Nan Wan, Bing Xiang Wang, Jin Hui Tao, Guo Jun Yang, Hai Feng Pan, and Jing Wang. 2012. "Matrix Metalloproteinases: A Review of Their Structure and Role in Systemic Sclerosis." *Journal of Clinical Immunology* 32 (6): 1409–14. https://doi.org/10.1007/s10875-012-9735-7.

Piao, Yin Ji, Hoe Suk Kim, and Woo Kyung Moon. 2019. "Noninvasive Photoacoustic Imaging of Dendritic Cell Stimulated with Tumor Cell-Derived Exosome." *Molecular Imaging and Biology*, August. https://doi.org/10.1007/s11307-019-01410-w.

Poincioux, Renaud, Floria Lizárraga, and Philippe Chavrier. 2009. "Matrix Invasion by Tumour Cells: A Focus on MT1-MMP Trafficking to Invadopodia." *Journal of Cell Science* 122 (17): 3015–24. https://doi.org/10.1242/jcs.034561.

Radisky, Evette S., and Derek C. Radisky. 2010. "Matrix Metalloproteinase-Induced Epithelial-Mesenchymal Transition in Breast Cancer." *Journal of Mammary Gland Biology and Neoplasia* 15 (2): 201–12. https://doi.org/10.1007/s10911-010-9177-x.

———. 2015. "Matrix Metalloproteinases as Breast Cancer Drivers and Therapeutic Targets." *Frontiers in Bioscience - Landmark* 20 (7): 1144–63. https://doi.org/10.2741/4364.

Rak, Janusz. 2013. "Extracellular Vesicles - Biomarkers and Effectors of the Cellular Interactome in Cancer." *Frontiers in Pharmacology* 4 (21). https://doi.org/10.3389/fphar.2013.00021.

Rak, Janusz, and Abhijit Guha. 2012. "Extracellular Vesicles – Vehicles That Spread Cancer Genes." *BioEssays* 34 (6): 489–97. https://doi.org/10.1002/bies.201100169.

Rangaraju, Srikant, Keith K Khoo, Zhi-Ping Feng, George Crossley, Daniel Nugent, Ilya Khaytin, Victor Chi, et al. 2010. "Potassium Channel Modulation by a Toxin Domain in Matrix Metalloprotease 23." *The Journal of Biological Chemistry* 285 (12): 9124–36. https://doi.org/10.1074/jbc.M109.071266.

Raposo, Graça Graca Graça, and Willem Stoorvogel. 2013. "Extracellular Vesicles: Exosomes, Microvesicles, and Friends." *Journal of Cell Biology* 200 (4): 373–83. https://doi.org/10.1083/jcb.201211138.

Ravanti, L., and V. M. Kähäri. 2000. "Matrix Metalloproteinases in Wound Repair (Review)." *International Journal of Molecular Medicine* 391-798. https://doi.org/10.3892/ijmm.6.4.391.

Reiner, Agnes T., Sisareuth Tan, Christiane Agreiter, Katharina Auer, Anna Bachmayr-Heyda, Stefanie Aust, Nina Pecha, et al. 2017. "EV-Associated MMP9 in High-Grade Serous Ovarian Cancer Is Preferentially Localized to Annexin V-Binding EVs." *Disease Markers* 2017: 9653194. https://doi.org/10.1155/2017/9653194.

Rorive, Sandrine, Alix Berton, Nicky D'haene, Constantin Nicolae Takacs, Olivier Debeir, Christine Decaestecker, and Isabelle Salmon. 2008. "Matrix Metalloproteinase-9 Interplays with the IGFBP2-IGFII Complex to Promote Cell Growth and Motility in Astrocytomas." *GLIA* 56 (15): 1679–90. https://doi.org/10.1002/glia.20719.

Sadowski, T., S. Dietrich, F. Koschinsky, A. Ludwig, E. Proksch, B. Titz, and R. Sedlacek. 2005. "Matrix Metalloproteinase 19 Processes the Laminin 5 Gamma 2 Chain and Induces Epithelial Cell Migration." *Cellular and Molecular Life Sciences* 62 (7–8): 870–80. https://doi.org/10.1007/s00018-005-4478-8.

Sakata, Keita, Ken-ichi Kozaki, Ken-ichi Iida, Rie Tanaka, Sadako Yamagata, Kazuhiko R. Utsumi, Shinsuke Saga, Satoru Shimizu, and Mutsushi Matsuyama. 1996. "Establishment and Characterization of High- and Low-lung-metastatic Cell Lines Derived from Murine Colon Adenocarcinoma 26 Tumor Line." *Japanese Journal of Cancer Research : Gann* 87 (1): 78–85. https://doi.org/10.1111/j.1349-7006.1996.tb00203.x.

Sánchez, Catherine A., Eliana I. Andahur, Rodrigo Valenzuela, Enrique A. Castellón, Juan A. Fullá, Christian G. Ramos, and Juan C. Triviño. 2016. "Exosomes from Bulk and Stem Cells from Human Prostate Cancer Have a Differential MicroRNA Content That Contributes Cooperatively over Local and Pre-Metastatic Niche." *Oncotarget* 7 (4): 3993–4008. https://doi.org/10.18632/oncotarget.6540.

Schmidt, Johannes R., Stefanie Kliemt, Carolin Preissler, Stephanie Moeller, Martin Von Bergen, Ute Hempel, and Stefan Kalkhof. 2016. "Osteoblast-Released Matrix Vesicles, Regulation of Activity and Composition by Sulfated and Non-Sulfated Glycosaminoglycans." *Molecular and Cellular Proteomics* 15 (2): 558–72. https://doi.org/10.1074/mcp.M115.049718.

Schumaker, Verne. 1994. *Lipoproteins, Apolipoproteins, and Lipases.* 1st ed. Vol. 45. Academic Press. https://www.elsevier.com/books/lipoproteins-apolipoproteins-and-lipases/anfinsen/978-0-12-034245-7.

Shimoda, Masayuki, and Rama Khokha. 2013. "Proteolytic Factors in Exosomes." *Proteomics* 13 (10–11): 1624–36. https://doi.org/10.1002/pmic.201200458.

Shipley, J M, G A Doyle, C J Fliszar, Q Z Ye, L L Johnson, S D Shapiro, H G Welgus, and R M Senior. 1996. "The Structural Basis for the Elastolytic Activity of the 92-KDa and 72-KDa Gelatinases. Role of the Fibronectin Type II-like Repeats."

The Journal of Biological Chemistry 271 (8): 4335–41. https://doi.org/10.1074/jbc.271.8.4335.

Simpson, Richard J., Justin W.E. Lim, Robert L. Moritz, and Suresh Mathivanan. 2009. "Exosomes: Proteomic Insights and Diagnostic Potential." *Expert Review of Proteomics* 6 (3): 267-83. https://doi.org/10.1586/epr.09.17.

Sogawa, Chiharu, Takanori Eguchi, Yuka Okusha, Kisho Ono, Kazumi Ohyama, Motoharu Iizuka, Ryu Kawasaki, et al. 2019. "A Reporter System Evaluates Tumorigenesis, Metastasis, β-Catenin/MMP Regulation, and Druggability." *Tissue Engineering. Part A* 25 (19–20): 1413–25. https://doi.org/10.1089/ten.TEA.2018.0348.

Sogawa, Chiharu, Takanori Eguchi, Manh Tien Tran, Masayuki Ishige, Kilian Trin, Yuka Okusha, Eman Ahmed Taha, et al. 2020. "Antiparkinson Drug Benztropine Suppresses Tumor Growth, Circulating Tumor Cells, and Metastasis by Acting on SLC6A3/DAT and Reducing STAT3." *Cancers* 12 (2). https://doi.org/10.3390/cancers12020523.

Steffensen, B, U M Wallon, and C M Overall. 1995. "Extracellular Matrix Binding Properties of Recombinant Fibronectin Type II-like Modules of Human 72-KDa Gelatinase/Type IV Collagenase. High Affinity Binding to Native Type I Collagen but Not Native Type IV Collagen." *The Journal of Biological Chemistry* 270 (19): 11555–66. https://doi.org/10.1074/jbc.270.19.11555.

Sternlicht, Mark D., and Zena Werb. 2001. "How Matrix Metalloproteinases Regulate Cell Behavior." *Annual Review of Cell and Developmental Biology* 17 (1): 463–516. https://doi.org/10.1146/annurev.cellbio.17.1.463.

Suzuki, Masashi, Gerhard Raab, Marsha A. Moses, Cecilia A. Fernandez, and Michael Klagsbrun. 1997. "Matrix Metalloproteinase-3 Releases Active Heparin-Binding EGF-like Growth Factor by Cleavage at a Specific Juxtamembrane Site." *Journal of Biological Chemistry* 272 (50): 31730–37. https://doi.org/10.1074/jbc.272.50.31730.

Svensson, Katrin J., Helena C. Christianson, Anders Wittrup, Erika Bourseau-Guilmain, Eva Lindqvist, Lena M. Svensson, Matthias Mörgelin, and Mattias Belting. 2013. "Exosome Uptake Depends on ERK1/2-Heat Shock Protein 27 Signaling

and Lipid Raft-Mediated Endocytosis Negatively Regulated by Caveolin-1." *Journal of Biological Chemistry* 288 (24): 17713–24. https://doi.org/10.1074/jbc.M112.445403.

Szatanek, Rafał, Monika Baj-Krzyworzeka, Jakub Zimoch, Małgorzata Lekka, Maciej Siedlar, and Jarek Baran. 2017. "The Methods of Choice for Extracellular Vesicles (EVs) Characterization." *International Journal of Molecular Sciences* 18 (6), 1153. https://doi.org/10.3390/ijms18061153.

Taha, E.A., Chiharu Sogawa, Yuka Okusha, Hotaka Kawai, Ayano Satoh, Kuniaki Okamoto, and T. Eguchi. n.d. *Okayama University, Okayama, Japan.*

Taha, Eman A, Kisho Ono, and Takanori Eguchi. 2019. "Roles of Extracellular HSPs as Biomarkers in Immune Surveillance and Immune Evasion." *International Journal of Molecular Sciences* 20 (18): 4588. doi: 10.3390/ijms20184588.

Takafuji, V., M. Forgues, E. Unsworth, P. Goldsmith, and X. W. Wang. 2007. "An Osteopontin Fragment Is Essential for Tumor Cell Invasion in Hepatocellular Carcinoma." *Oncogene* 26 (44): 6361–71. https://doi.org/10.1038/sj.onc.1210463.

Tamkovich, S. N., O. S. Tutanov, and P. P. Laktionov. 2016. "Exosomes: Generation, Structure, Transport, Biological Activity, and Diagnostic Application." *Biochemistry (Moscow) Supplement Series A: Membrane and Cell Biology 10 (3): 163-73.* https://doi.org/10.1134/S1990747816020112.

Taraboletti, Giulia, Sandra D'Ascenzo, Patrizia Borsotti, Raffaella Giavazzi, Antonio Pavan, and Vincenza Dolo. 2002. "Shedding of the Matrix Metalloproteinases MMP-2, MMP-9, and MT1-MMP as Membrane Vesicle-Associated Components by Endothelial Cells." *The American Journal of Pathology* 160 (2): 673–80.

Théry, Clotilde, Muriel Boussac, Philippe Véron, Paola Ricciardi-Castagnoli, Graça Raposo, Jerôme Garin, and Sebastian Amigorena. 2001. "Proteomic Analysis of Dendritic Cell-Derived Exosomes: A Secreted Subcellular Compartment Distinct from Apoptotic Vesicles." *The Journal of Immunology* 166 (12): 7309–18. https://doi.org/10.4049/jimmunol.166.12.7309.

Théry, Clotilde, Matias Ostrowski, and Elodie Segura. 2009. "Membrane Vesicles as Conveyors of Immune Responses." *Nature Reviews. Immunology* 9 (8): 581–93. https://doi.org/10.1038/nri2567.

Théry, Clotilde, Kenneth W. Witwer, Elena Aikawa, Maria Jose Alcaraz, Johnathon D. Anderson, Ramaroson Andriantsitohaina, Anna Antoniou, et al. 2018. "Minimal Information for Studies of Extracellular Vesicles 2018 (MISEV2018): A Position Statement of the International Society for Extracellular Vesicles and Update of the MISEV2014 Guidelines." *Journal of Extracellular Vesicles* 7 (1). https://doi.org/10.1080/20013078.2018.1535750.

Tovar-Camargo, Oscar A., Shusuke Toden, and Ajay Goel. 2016. "Exosomal MicroRNA Biomarkers: Emerging Frontiers in Colorectal and Other Human Cancers." *Expert Review of Molecular Diagnostics* 16 (5): 553–67. https://doi.org/10.1586/14737159.2016.1156535.

Trajkovic, Katarina, Chieh Hsu, Salvatore Chiantia, Lawrence Rajendran, Dirk Wenzel, Felix Wieland, Petra Schwille, Britta Brügger, and Mikael Simons. 2008. "Ceramide Triggers Budding of Exosome Vesicles into Multivesicular Endosomes." *Science* 319 (5867): 1244–47. https://doi.org/10.1126/science.1153124.

Triola, Gemma, Herbert Waldmann, and Christian Hedberg. 2012. "Chemical Biology of Lipidated Proteins." *ACS Chemical Biology* 7 (6): 1015-22. https://doi.org/10.1021/cb200460u.

Vagner, Tatyana, Cristiana Spinelli, Valentina R. Minciacchi, Leonora Balaj, Mandana Zandian, Andrew Conley, Andries Zijlstra, et al. 2018. "Large Extracellular Vesicles Carry Most of the Tumour DNA Circulating in Prostate Cancer Patient Plasma." *Journal of Extracellular Vesicles* 7 (1): 1505403. https://doi.org/10.1080/20013078.2018.1505403.

Venning, Freja A, Lena Wullkopf, and Janine T Erler. 2015. "Targeting ECM Disrupts Cancer Progression." *Frontiers in Oncology* 5: 224. https://doi.org/10.3389/fonc.2015.00224.

Verpelli, Chiara, Michael J. Schmeisser, Carlo Sala, and Tobias M. Boeckers. 2012. "Scaffold Proteins at the Postsynaptic Density." *Advances in Experimental Medicine and Biology* 970: 29–61. https://doi.org/10.1007/978-3-7091-0932-8_2.

Visse, Robert, and Hideaki Nagase. 2003. "Matrix Metalloproteinases and Tissue Inhibitors of Metalloproteinases: Structure, Function, and Biochemistry." *Circulation Research* 92 (8) 827-39. https://doi.org/10.1161/01.RES.0000070112.80711.3D.

Walker, N. I., B. V. Harmon, G. C. Gobé, and J. F. Kerr. 1988. "Patterns of Cell Death." *Methods and Achievements in Experimental Pathology* 13: 18–54.

Wang, Jiaoli, Yilei Wu, Jufeng Guo, Xuefeng Fei, Lei Yu, and Shenglin Ma. 2017. "Adipocyte-Derived Exosomes Promote Lung Cancer Metastasis by Increasing MMP9 Activity via Transferring MMP3 to Lung Cancer Cells." *Oncotarget* 8 (47): 81880–91. https://doi.org/10.18632/oncotarget.18737.

Webber, J. P., L. K. Spary, A. J. Sanders, R. Chowdhury, W. G. Jiang, R. Steadman, J. Wymant, et al. 2015. "Differentiation of Tumour-Promoting Stromal Myofibroblasts by Cancer Exosomes." *Oncogene* 34 (3): 290–302. https://doi.org/10.1038/onc.2013.560.

Xing, Fei, Jamila Saidou, and Kounosuke Watabe. 2010. "Cancer Associated Fibroblasts (CAFs) in Tumor Microenvironment." *Frontiers in Bioscience* 15 (January): 166–79.

Xu, Weifeng. 2011. "PSD-95-like Membrane Associated Guanylate Kinases (PSD-MAGUKs) and Synaptic Plasticity." *Current Opinion in Neurobiology* 21 (2): 306-12. https://doi.org/10.1016/j.conb.2011.03.001.

Y, Okada, Nagase H, and Harris ED Jr. 1987. "Matrix Metalloproteinases 1, 2, and 3 from Rheumatoid Synovial Cells Are Sufficient to Destroy Joints." *The Journal of Rheumatology* 14 (May): 41–42.

Yáñez-Mó, María, Pia R.-M. R.M. R-M Siljander, Zoraida Andreu, Apolonija Bedina Zavec, Francesc E. Borràs, Edit I. Buzas, Krisztina Buzas, et al. 2015. "Biological Properties of Extracellular Vesicles and Their Physiological Functions." *Journal of Extracellular Vesicles* 4 (2015): 27066. https://doi.org/10.3402/jev.v4.27066.

Yang, Feng, Jennifer A. Tuxhorn, Steven J. Ressler, Stephanie J. McAlhany, Truong D. Dang, and David R. Rowley. 2005. "Stromal Expression of Connective Tissue Growth Factor Promotes Angiogenesis and Prostate Cancer Tumorigenesis."

Cancer Research 65 (19): 8887–95. https://doi.org/10.1158/0008-5472.CAN-05-1702.

Yang, Xiuwei, Oleg V. Kovalenko, Wei Tang, Christoph Claas, Christopher S. Stipp, and Martin E. Hemler. 2004. "Palmitoylation Supports Assembly and Function of Integrin–Tetraspanin Complexes." *The Journal of Cell Biology* 167 (6): 1231–40. https://doi.org/10.1083/jcb.200404100.

Yin, Dong, Weikai Chen, James O'Kelly, Daning Lu, Michelle Ham, Ngan B Doan, Dong Xie, et al. 2010. "CTGF Associated with Oncogenic Activities and Drug Resistance in Glioblastoma Multiforme (GBM)." *International Journal of Cancer* 127 (10): 2257–67. https://doi.org/10.1002/ijc.25257.

Yokoi, Akira, Yusuke Yoshioka, and Takahiro Ochiya. 2015. "Towards the Realization of Clinical Extracellular Vesicle Diagnostics: Challenges and Opportunities." *Expert Review of Molecular Diagnostics* 15 (12): 1555–66. https://doi.org/10.1586/14737159.2015.1104249.

Yoshida, Saori, Hotaka Kawai, Takanori Eguchi, Shintaro Sukegawa, May Wathone Oo, Chang Anqi, Kiyofumi Takabatake, Keisuke Nakano, Kuniaki Okamoto, and Hitoshi Nagatsuka. 2019. "Tumor Angiogenic Inhibition Triggered Necrosis (TAITN) in Oral Cancer." *Cells* 8 (7). https://doi.org/10.3390/cells8070761.

Yoshii, Yukie, Atsuo Waki, Kaori Yoshida, Anna Kakezuka, Maki Kobayashi, Hideo Namiki, Yusei Kuroda, et al. 2011. "The Use of Nanoimprinted Scaffolds as 3D Culture Models to Facilitate Spontaneous Tumor Cell Migration and Well-Regulated Spheroid Formation." *Biomaterials* 32 (26): 6052–58. https://doi.org/10.1016/j.biomaterials.2011.04.076.

Yoshimura, Aya, Masaki Kawamata, Yusuke Yoshioka, Takeshi Katsuda, Hisae Kikuchi, Yoshitaka Nagai, Naoki Adachi, et al. 2016. "Generation of a Novel Transgenic Rat Model for Tracing Extracellular Vesicles in Body Fluids." *Scientific Reports* 6 (August): 31172. https://doi.org/10.1038/srep31172.

Yoshioka, Yusuke, Yuki Konishi, Nobuyoshi Kosaka, Takeshi Katsuda, Takashi Kato, and Takahiro Ochiya. 2013. "Comparative Marker Analysis of Extracellular Vesicles in

Different Human Cancer Types." *Journal of Extracellular Vesicles* 2 (1): 20424. https://doi.org/10.3402/jev.v2i0.20424.

You, Yiwen, Ying Shan, Jing Chen, Huijun Yue, Bo You, Si Shi, Xingyu Li, and Xiaolei Cao. 2015. "Matrix Metalloproteinase 13-Containing Exosomes Promote Nasopharyngeal Carcinoma Metastasis." *Cancer Science* 106 (12): 1669–77. https://doi.org/10.1111/cas.12818.

Zaborowski, Mikołaj P, Leonora Balaj, Xandra O Breakefield, and Charles P Lai. 2015. "Extracellular Vesicles: Composition, Biological Relevance, and Methods of Study." *BioScience* 65 (8). https://doi.org/10.1093/biosci/biv084.

Zaborowski, Mikołaj Piotr, Kyungheon Lee, Young Jeong Na, Alessandro Sammarco, Xuan Zhang, Marcin Iwanicki, Pike See Cheah, et al. 2019. "Methods for Systematic Identification of Membrane Proteins for Specific Capture of Cancer-Derived Extracellular Vesicles." *Cell Reports* 27 (1): 255-268.e6. https://doi.org/10.1016/j.celrep.2019.03.003.

Zacharias, David A., Jonathan D. Violin, Alexandra C. Newton, and Roger Y. Tsien. 2002. "Partitioning of Lipid-Modified Monomeric GFPs into Membrane Microdomains of Live Cells." *Science* 296 (5569): 913–16. https://doi.org/10.1126/science.1068539.

Zuber, Mauricio X., Stephen M. Strittmatter, and Mark C. Fishman. 1989. "A Membrane-Targeting Signal in the Amino Terminus of the Neuronal Protein GAP-43." *Nature* 341 (6240): 345–48. https://doi.org/10.1038/341345a0.